Modeling the Thermal Stability of *in vitro* Diagnostic Bioassays

By

Stephen Lee Snyder

A thesis submitted to the Department of Chemical Engineering
in conformity with the requirements for the degree of
Master of Applied Science

Queen's University
Kingston, Ontario, Canada
(January, 2011)

Abstract

The objective of this work is to develop mathematical models for predicting the thermal stability of commercial diagnostic assays. These assays are a product of the Point of Care division of Abbott Laboratories, and are used for analyzing patient blood samples for specific substances. The accuracy of the results from these diagnostic tests relies on the activity of specific biological and/or chemical components of the sensors. Mathematical models that describe the stability of these active components are useful for supporting product shelf-life claims and for the design and implementation of accelerated testing protocols. In the thesis, the stability of two diagnostic assay systems of interest to Abbott Point of Care is investigated using mathematical modeling.

For the first assay system investigated, the biosensor associated with the assay is identified as an important factor for product stability. A second-order dynamic model is developed to describe the thermal stability of this biosensor. The model corresponds to a reversible reaction followed by an irreversible reaction, with rate coefficients having Arrhenius temperature dependencies. The second-order dynamic model provides improved predictions relative to a first-order dynamic model, based on a comparison between model fits for two experimental datasets, and a comparison of predictive ability for a validation dataset. The second-order dynamic model is used to extend the concept of Mean Kinetic Temperature concept from the pharmaceutical industry to systems with higher-order dynamics.

For the second assay system investigated, the calibration fluid is identified as a key factor in assay stability. A first-order model is developed to describe the stability of the analyte within the calibration fluid. The first-order model captures most of the trend present in the data from calibration fluid incubation experiments. Finally, model predictions are used to investigate the amount of change in assay response that can be attributed to changes in concentration of analyte in the calibration fluid (after storage at elevated temperatures). The results show that the changes observed in assay responses are consistent with the magnitude of changes in calibrant analyte concentrations predicted by the model.

Co-authorship

The material in Chapter 2 has been submitted to the refereed journal "Sensors and Actuators B: Chemical". I prepared the drafts of the manuscript, performed all of the calculations, ran all of the related simulations and generated all of the Figures and Tables. Dr. Kim McAuley, Dr. James McLellan, Dr. Eric Brouwer and Tamara McCaw are co-authors of the paper. They provided technical advice throughout the course of this work, helping to determine the direction and scope of the research undertaken, as well as editing the paper and thesis for clarity and for the protection of Abbott's intellectual property. Kim McAuley and James McLellan were active participants in discussions with me concerning modeling approaches and the analysis and interpretation of the data. Eric Brouwer and Tamara McCaw were instrumental in identifying the key assays to be investigated and providing a wealth of experimental data for analysis, prior to the design of my own experimental data sets.

Acknowledgements

I would like to thank Dr. Kim McAuley, Dr. James McLellan, Dr. Eric Brouwer and Tamara McCaw for their support, guidance and mentorship during my graduate studies. I have been extremely fortunate to have such enthusiastic, knowledgeable and caring supervisors.

My interactions with research scientists, managers and technicians at Abbott Point of Care have been memorable and extremely helpful. I would like to specifically thank Craig Jeffery, James Smith, Doug Borris, Glen Martin, Pamela Frank and Bill Keogh for all of the time that they spent bringing me up to date on APOC systems. I would additionally like to thank all of the members of the Abbott team who helped out at different stages of this project.

The companionship of my colleagues in the chemical engineering department has been a source of enjoyment during this work. I would especially like to thank all of my lab-mates for their help on numerous occasions with a variety of problems. I need to specifically thank Duncan Thompson, Shaohua (Roy) Wu, Hui Yuan, Jonathan Chain, John Woloszyn and Angelica Bitton, for all of the troubleshooting sessions, great discussions and for making graduate school such a memorable experience.

I would also like to thank Abbott Point of Care, Queen's University, MITACS and NSERC for this great opportunity and their financial support.

Finally, I would like to thank my parents and my brother, my most important teachers and companions, for all of their support and encouragement.

Table of Contents

List of Tables

List of Figures

Chapter 1: Introduction

1.1   Problem Description

Abbott Point of Care (APOC) manufactures single-use blood diagnostic assay cartridges for use with their i-STAT® handheld analyzer. A blood sample from a patient is deposited into the sample entry well of the cartridge and the cartridge is inserted into the APOC i-STAT analyzer. The analyzer then performs an automated sequence whereby the biosensor chips take readings of both a calibration fluid (from a calibration pouch) and the blood sample. A diagram of a representative cartridge and its components is included as Figure 1.1.
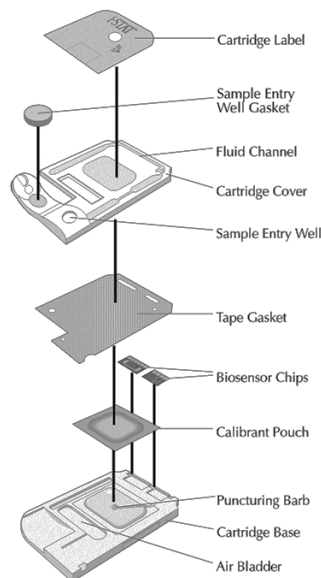
Figure 1.1: Exploded view of an APOC i-STAT cartridge (figure used with permission from APOC)

The APOC i-STAT assay cartridges contain chemical and biological components. The stability of the chemical and biological components limits the shelf-life of these assay products, and imposes specific requirements for storage at cold to moderate temperatures.

To improve product stability and extend the current shelf-life claims, APOC actively investigates the stability of the chemical and biological components of their assay cartridges. This thesis focuses on the development of stability models for components of the diagnostic assay cartridges. Stability models allow for shelf-life predictions and for extrapolation from accelerated testing experiments. These models can be used to simulate product responses, establish hypotheses, design experiments or perform sensitivity analyses. The model development process involves exploring relationships between stress factors and product performance over time; the understanding of these relationships is a valuable for scientific and product quality advances.

1.2   *Electrochemical Sensors and Biosensors*

Traditional electrochemical sensors for use in clinical chemistry can be classified into two main categories; potentiometric sensors or amperometric sensors. In potentiometric sensors, a potential difference is measured between an indicator electrode and a reference electrode, both in contact with the testing solution. The potential generated across the two electrodes is proportional to the logarithm of analyte concentration in the sample. [1.2]

For amperometric sensors, an electrical potential is applied across the working and reference electrodes, to drive redox reactions in the solution that separates them. The analyte of interest is a participant in the redox reaction(s) that occur in the solution, and the flow of electrical current that results from the applied potential is proportional to the concentration of analyte present [1.2].

Biosensors are electrochemical sensors (either potentiometric or amperometric) containing a biological component that interacts selectively with an analyte of interest in a testing sample. This interaction produces effects that are translated into a readily measurable

2

form, such as an electrical signal, by a transducer element [1.3]. A coupled enzyme-electrode system is an example of a biosensor. This form of biosensor consists of an enzyme immobilized in a polymer matrix at the surface of an electrode. When the immobilized enzyme interacts with the analyte of interest, a change in a property of the surrounding solution is produced, which is converted into a quantifiable electrical signal [1.3]. Enzymes that catalyze transformations of specific biological molecules can be used in this setup to detect the presence and quantity of those biological molecules in samples of interest.

The relationship between the electrical signal measured from the transducer element and the presence, activity or concentration of the targeted analyte in the sample is not always a linear one. In many cases, a mathematical model is required to relate the electrical signal observed to the property measured, for accurate quantification. A variety of models have been developed for potentiometric sensors [1.4], enzyme-based amperometric biosensor systems [1.5], mass-sensitive chemical sensor systems [1.5,1.6] and optical biosensors [1.7-1.9]. These models typically incorporate concepts from thermodynamics, mass transport phenomena and electrochemistry to describe the behaviour of the biosensor system, but may also include some empirical or semi-empirical model components for system calibration.

1.3 Diagnostic Assay Stability

Changes to the diagnostic assay system of interest over time may introduce a bias in the mathematical model that calculates the analytical value from the raw sensor response. It is important, therefore, for assay manufacturers to be aware of the lifetime of their products and of the influence that both typical and atypical storage conditions may have on assay performance. Monitoring of assay responses to identify changes in assay stability is a basic method for manufacturers to track changes in product performance. To monitor product

performance under specified storage conditions, assay cartridges from the same production lot are regularly tested for their response to a control fluid with known analyte concentrations. For single-use diagnostic assays, this monitoring represents destructive testing. Ideally, the responses of diagnostic assay cartridges from the same lot to the same control fluid should be identical, but in practice the outcomes from several tests form a distribution of responses. The mean of the distribution should correspond to the true concentration of the analyte in the control fluid, within specified error allowances. For APOC devices sold to clients in the United States of America, tolerances for the error in the measured analytical values are established based on the standards set by the Clinical Laboratory Improvement Amendments (CLIA) program. The CLIA program outlines a level of medically allowable error specific to each analyte of clinical interest and is run by the Centers for Medicare and Medicaid Services (CMS) agency of the United States Department of Health and Human Services (DHHS). [1.1]

To assess assay stability, the characteristics of this distribution of responses must be investigated over time and after exposure to different storage conditions. There are three main stability issues that can be detected through this approach: changes in the mean response, changes in the variance of the response, and changes in the frequency of outright product failures (where no meaningful response can be generated). If changes in one or more of these statistics are detected, efforts are made to identify the causes of the changes, and to investigate their impact on assay stability. Accelerated testing experiments can be helpful in cases where the long-term stability of a sensor system needs to be investigated in a short time period.

1.4 Accelerated Testing and Stability Modeling

An extensive review of accelerated testing theory and methodology was performed by Meeker and Escobar [1.11]. The variety of accelerated testing approaches, applications and associated theories is vast, and spans many different manufacturing sectors [1.11]. The purpose of this section, therefore, is not to provide an in-depth review of the accelerated testing literature, but rather to provide a brief summary of accelerated testing goals and approaches as they pertain to the development of stability predictions for electrochemical sensors with biological and chemical components.

In the context of this thesis, accelerated testing involves subjecting a system to higher stress than would be experienced during normal operation, in order to observe changes that would normally take much longer to occur under milder conditions. In many systems, mathematical models allow for extrapolation from accelerated testing regimes to normal operating conditions, so that the duration of stability experiments can be shortened [1.11]. Results from experiments that expose the product or system of interest to high levels of stress can be used to estimate the parameters for the stability model of the system, and the model can subsequently be used to predict system behaviour under alternative levels of stress. Ideally, stability models for a biological or chemical system should be fundamental models, derived from the basic thermodynamic, mass-transport and chemical kinetics of the system. In practice, the cost (in terms of both time and resources) of experimentation to investigate each component of a fundamental system for a complex process may be prohibitive, and an empirical or semi-empirical model must suffice for approximating the stability of the system [1.12].

Accelerated testing approaches are highly desirable when decisions about a product cannot feasibly wait for a full-scale, long-term study [1.13]. The application of accelerated testing methodology to the food, pharmaceutical and other industries that deal with biological and chemical components is well established for the prediction of product shelf-life. The quality of products with active biological components is typically defined in terms of biological function, and product expiration specifications are set based on maximum allowable percentage losses in activity over time, under explicit storage conditions [1.13]. For typical pharmaceutical applications, the shelf-life is interpreted as the time at which the lower 95% confidence bound for the regression line of product activity (at an isothermal storage temperature) crosses below a 90% drug potency threshold [1.14]. While it is possible to perform real-time testing on pharmaceutical products to establish shelf-life estimates, it is of interest to experiment with short-term exposures of product samples to elevated humidity, temperature or other important factors that influence product stability, and then to extrapolate a shelf-life estimate for normal storage conditions from the experimental results. From the above description of accelerated testing methods and applications, there are four points that are especially relevant to subsequent chapters of this work:

1. Accelerated testing approaches are an effective method for quickly characterizing product shelf-life and designing experiments that test between product design alternatives in a timely manner.

2. The ability to use accelerated test results for extrapolation relies on a stability model for the system of interest that provides a description of the stability behaviour over the ranges and durations of stresses experienced.

3. Stability models are ideally fundamental models, but in practice empirical or semi-empirical stability models are more frequently available as approximations of the system.

4. The use of accelerated testing methods is common in industries where products contain bioactive components; examples being the pharmaceutical and food industries.

1.5   *Objectives and Thesis Outline*

The objectives of this thesis are to develop stability models and to estimate parameters for two of the APOC diagnostic assay systems. The development of these models involves: the analysis of available APOC data concerning the systems of interest; the formulation of mathematical models to describe the behaviour of the systems; the fitting of model parameters to the available data; and the design of experiments to generate new data sets for improved parameter estimation and model validation, as necessary. The remainder of this thesis is organized into three chapters. Chapter 2 describes the development of a semi-empirical, second-order dynamic model to predict the stability of a particular APOC biosensor used to measure an analyte in human blood. This chapter has been prepared as a journal article for submission to *Sensors and Actuators B*: *Chemical.* Chapter 3 presents the development of a first-order stability model for an analyte present in the calibration package of a second type of APOC sensor.   Finally, Chapter 4 provides a summary of the conclusions drawn from this work, and indicates the novel aspects of the research.

1.6 References (Chapter 1)

[1.1] Clinical Laboratory Improvement Amendments (CLIA), Centers for Medicare and Medicaid Services, U.S. Department of Health and Human Services. Accessed online: December, 2010. Web Address: http://www.cms.gov/clia/

[1.2] J.D. Czaban, Electrochemical sensors in clinical chemistry: yesterday, today, tomorrow, Anal. Chem. 57:2 (1985) A345

[1.3] P. d'Orazio, Biosensors in clinical chemistry, Clin. Chim. Acta 334 (2003) 41-69.

[1.4] J. Bobacka, A. Ivaska and A. Lewenstam, Potentiometric ion sensors, Chem. Rev. 108:2 (2008) 329-351.

[1.5] P.N. Bartlett and K.F.E. Pratt, Modeling of processes in enzyme electrodes, Biosens. Bioelectron. 8 (1993) 451-462.

[1.6] P. Boeker, O. Wallenfang and G. Horner, Mechanistic model of diffusion and reaction in thin sensor layers – the DIRMAS model, Sens. Actuators B 83 (2002) 202-208.

[1.7] F. Thalmayr and G. Fischerauer, Sensor signal processing for gravimetric chemical sensors based on a state-space model, Sens. Actuators B 144 (2010) 27-36.

[1.8] Y.G. Tsay et al, Optical Biosensor Assay, Clin. Chem. 37:9 (1991) 1502-1505.

[1.9] C. Domenici et al., Development of a TIRF immunosensor: modelling the equilibrium behaviour of a competitive system, Biosens. Bioelectron. 10 (1995) 371-378.

[1.10] J.Q. Brown, M.J. McShane, Modeling of spherical fluorescent glucose microsensor systems: Design of enzymatic smart tattoos, Biosens. Bioelectron. 21 (2006) 1760-1769.

[1.11] W.Q. Meeker and L.A. Escobar, A review of recent research and current issues in accelerated testing, Int. Stat. Rev. 61 (1993) 147-168.

[1.12] M.J. LuValle, An approximate kinetic theory for accelerated testing, Inst. Ind. Eng. Trans. 31 (1999) 1147-1156.

[1.13] F. Franks, Accelerated stability testing of bioproducts: attractions and pitfalls, Trend. Biotech. 12 (1994) 114-117.

[1.14] B. Kommanaboyina and C.T. Rhodes, Effects of temperature excursions on mean kinetic temperature and shelf life, Drug Dev. Ind. Pharm. 25 (1999) 1301-1306.

Chapter 2: Modeling the Thermal Stability of Enzyme-Based Biosensors

2.0 Abstract

Performance of *in vitro* diagnostics biosensors may change over lifetime, particularly if environmental storage conditions such as temperature are not controlled. Biosensors are composed of diverse multiple components such as salts, polymers and biological components which may be differentially impacted by chemical and physical transformations induced by changes in temperature and exposure to humidity, oxygen and light. Mathematical models for predicting the influence of temperature on biosensor performance over time typically assume the changes follow first-order dynamics, with the temperature dependence of the rate of change described by an Arrhenius kinetic expression. However, the compositional diversity found in many biosensors may cause the assumption of first-order dynamics for sensor stability to be invalid. In this paper, a second-order dynamic model is developed to predict the change in biosensor performance over time for a single-use biosensor used in a point-of-care diagnostics system. The model consists of a reversible reaction followed by an irreversible reaction, with rate coefficients having Arrhenius temperature dependencies. The second-order dynamic model provides improved predictions, based on a comparison for two experimental datasets used for estimation, and on a validation dataset. The resulting model has applications for shelf-life prediction, designing accelerated testing experiments, biosensor improvement and the development of biosensor storage guidelines. Finally, it is shown that the concept of "mean kinetic temperature", used widely in the pharmaceutical industry and based on first-order dynamics, can be applied successfully to a biosensor system exhibiting higher-order dynamic behaviour using a second-order model. This suggests that MKT concepts may be extended to *in vitro* diagnostics sensor applications.

2.1   Introduction

Conventional *in vitro* diagnostic analyses take place in medical laboratories that employ specialized equipment for analyzing biological samples from patients. The test results are forwarded to the clinician, often with an inherent processing delay. Advances in diagnostic technologies have led to the development of smaller, portable diagnostic systems that can eliminate time delays between the patient and laboratory by bringing the diagnostics system to the patient's side. This approach of analyzing samples at the site of the patient is referred to as "Point of Care" (POC) diagnostics. Since their introduction, POC diagnostic systems have become valuable tools for the modern medical practitioner [2.1].

In this article, we focus on single-use, in vitro diagnostic systems for analyzing blood at the patient point of care. Clinical POC diagnostic systems are currently available for measuring a variety of blood components including ion concentrations, blood gas partial pressures, pH levels, and concentrations of compounds such as urea, glucose, creatinine and lactate. Detection technologies may vary, but are typically based on optical or electrochemical principles [2.2].

A variety of mathematical models have been developed for simulating and characterizing responses from enzyme-based biosensors [2.3-2.6] and from gravimetric biosensors [2.7-2.9]. These mathematical models generally describe three main processes: the diffusive characteristics of the sensor layers, the kinetics of substrate/active site binding, and the electrochemical reaction kinetics at the electrode. The models have been used to improve sensor response time [2.7,2.8,2.4,2.9], to optimize important sensor design factors [2.3,2.7], or to identify conditions where the behaviour of the sensor changes [2.5].

Biosensor models are also necessary for converting the raw sensor response signal into an analytical value that quantifies the presence of analyte in the sample.

Unfortunately, biosensors are susceptible to changes in activity during storage, commonly due to the exposure of their components to stresses such as humidity, elevated temperature and oxygen [2.10,2.11]. After storage involving high levels of stress, the relationship between the raw biosensor response and the level of analyte present may deviate from the equation(s) used in the sensor, either in terms of the parameter values and/or the form of the response curve. This can make comparisons to the calibration standard difficult and introduce bias into the sensor readings computed from the raw signal.

Significant progress has been made over the past few decades in stabilizing enzyme-based biosensors using different enzyme-immobilization techniques [2.11,2.12]. While these techniques have extended the workable lifetime of enzyme-based biosensors to a state where they are commercially viable, stability concerns and room for improvement still exist [2.2,2.11], and biosensor shelf life remains an important performance consideration for manufacturers of these devices.

Similar shelf life stability challenges are faced by pharmaceutical companies whose drug products may be sensitive to temperature, pH, moisture, light and oxygen levels [2.13]. To address thermal exposure concerns, the pharmaceutical industry employs a "mean kinetic temperature" (MKT) method for predicting the temperature-dependent change in activity of products with chemically-active components [2.14]. The MKT is the equivalent temperature that produces a specified change in activity over a specified period of time. The rate of change is described by the Arrhenius equation widely used in chemical reaction kinetics:

$$k = A_0 e^{\frac{-E_a}{RT}}$$

$$= k_{ref} e^{\frac{-E_a}{R}\left(\frac{1}{T}-\frac{1}{T_{ref}}\right)}$$

$$(1)$$

The Arrhenius equation relates a reaction rate coefficient k, to the absolute temperature T. In equation (1), E_a is an activation energy, R is the universal gas constant, and A_0 is a pre-exponential factor. As shown above, the Arrhenius equation can be restated in terms of k_{ref} (instead of A_0), where k_{ref} is the value of the rate coefficient at a reference temperature T_{ref} [2.16]. T_{ref} is usually selected to be a typical temperature within the range of experimental temperatures of interest. This reparameterization has the benefit of improving the statistical quality of the estimates, and improving the conditioning of the estimation problem [2.16].

For many pharmaceutical products, it is common to assume first-order dynamics for changes in stability. This assumption is used for the development of regulatory standards involving pharmaceutical shelf-life predictions and monitoring [2.17]. The actual storage temperature is recorded by the pharmacist, allowing for the prediction of the product expiry date through the use of the calculated MKT based on the Arrhenius equation and the first-order dynamic model. The drug product may be deemed expired if the worst-case prediction of its activity level falls below 90% of its original target activity. This procedure for product expiration monitoring in the pharmaceutical industry helps to ensure the safety of patients through vigilant removal of expired products. As the *in vitro* diagnostics industry in general, and single-use point of care diagnostics in particular, encounters analogous product stability challenges, the methods implemented by the pharmaceutical industry could be adapted for single-use POC diagnostics applications.

12

First-order dynamic models incorporating an Arrhenius-type temperature dependency for the rate of change have already been used in the biosensor literature for evaluating sensor stability [2.17,2.18]. McAteer et al. [2.18] proposed a general model for biosensor shelf-life performance assuming a first-order dynamic process to describe biosensor aging, with temperature dependency based on the Arrhenius equation. While this approach may adequately approximate a biosensor containing a single thermally-sensitive component, it may be insufficient for more complex biosensors having multiple thermally-sensitive components. Thermally sensitive components may consist of a range of elements, including altered diffusive properties for the polymer matrix layers in the sensor, and/or altered activities for one or more enzymes present in the biosensor system. The combination of these types of changes could produce higher-order dynamic behaviour for biosensor stability, so that first-order models might inadequately describe such systems.

In the current paper, thermal stability data from Abbott Point of Care (APOC) biosensors are used to develop dynamic models for the stability of a particular biosensor product. Since detailed mechanistic knowledge of the thermally-induced aging pathways is unavailable, a semi-empirical dynamic modeling approach is developed using experimental data sets obtained using a variety of storage conditions. Preliminary fits using first-order models are shown to provide an inadequate prediction of the data, motivating the consideration of second-order dynamic models. Results obtained using a second-order differential-equation model are compared to those from a first-order model and a method is proposed for determining MKT using higher-order dynamic models of sensor stability.

2.2   *Materials and Methods*

2.2.1 Biosensor

Data from non-commercial single-use biosensors were obtained from Abbott Point of Care (Ottawa, Canada). The biosensor of interest consists of an electrode onto which polymeric layers containing bioactive components have been deposited.   Electrical response profiles generated by the electrode when in contact with samples, are directly related to the concentration of the analyte of interest in the sample. The extent of change in a thermally-aged biosensor was determined by testing samples of known analyte concentrations using thermally-aged biosensors. The activity of the sensor was tracked as the ratio of the response from the thermally-aged biosensor to that of the sensor at time = 0. Results for a given dataset were obtained from a single production lot.

2.2.2 Experimental data sets

Two experimental data sets were obtained to develop the model and estimate the model parameters. The first data set (Data Set A) contains time-series data for biosensors stored at four different temperature conditions spanning a range exceeding the thermal stress that these sensors would typically experience during shipment, use and storage. Perturbations to the storage temperature were introduced to represent poor storage conditions. These fluctuations do not reflect standard practice for product storage, and the product met performance expectations under the labeled use and storage guidelines. For each test event, multiple biosensors from each storage condition were used to analyze an aqueous control fluid with a known analyte concentration. The second source of data (Data Set B) involves biosensors stored at three different conditions, with temperatures spanning a range similar to that in Data Set A, but with less perturbation of the storage temperature. The

14

testing plan for data set B was developed to complement Data Set A, which was available from APOC experiments prior to the commencement of this work. As a result, several of the test events overlap between the two data sets to allow for meaningful comparison between mean response values. In addition, test events were scheduled to provide information about the regions of the changing response trajectory that was not available from Data Set A. A table showing the experimental plan for Data Sets A and B is included as Table B1 in Appendix B. Frequent temperature readings from the ovens used to store the biosensors were available for each data set, providing a detailed log of the thermal stress applied to the biosensors during storage.

A third experimental data set (Data Set C) was collected for model validation. Data Set C used step tests (Figure 2.1) to investigate the influence of dynamic temperature excursions to extremes of the temperature range spanned by Data Set A. Data Set C was used to test the predictive ability of the first- and second-order models, using parameter estimates generated by fitting Data Sets A and B. The experimental plan for Data Set C is included as Table B2 in Appendix B.
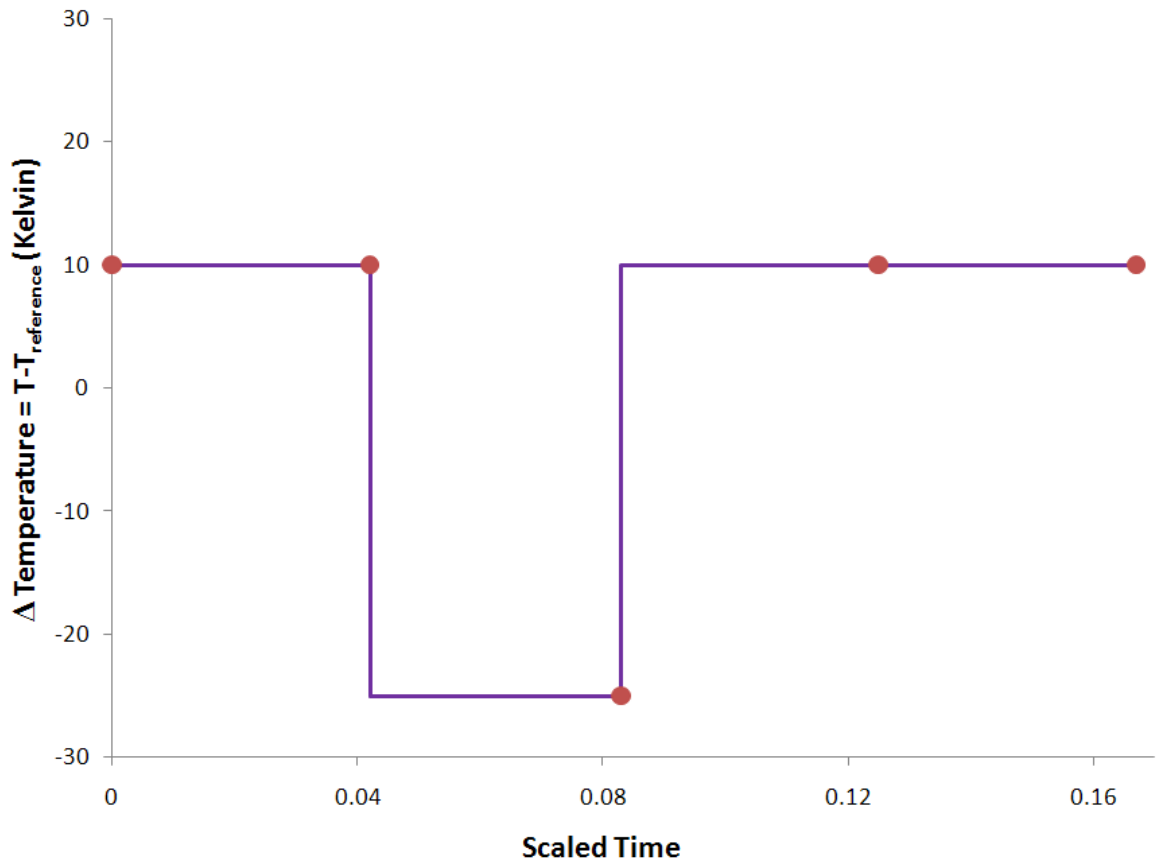
Figure 2.1: The solid line (—) shows the incubation plan for Data Set C and the circles (●) show the timing of the test events. The temperatures have been recoded relative to the nominal temperature associated with Storage Condition II. The time axis has been recoded as a fraction of the total duration of the Data Set A experiment.

2.2.3 Modeling approach

Developing a detailed fundamental dynamic model for the thermal stability of the biosensor requires knowledge of the sensing signal-pathway reactions and aging reactions associated with each step in the pathway. Additionally, the effects of thermal aging on the diffusion and other properties of each polymer layer in the bioactive film need to be understood. Due to the complexity of building a mechanistic model, and a lack of data on the detailed behaviour of the biosensor system under thermal aging conditions, a simplified,

16

semi-empirical approach was used to develop models describing the thermal stability of the biosensors.

Initially, a first-order dynamic model was used to describe the system. Subsequently, a more complex second-order dynamic model was developed using lumped reaction-rate and activation-energy terms to approximate the true higher-order aging processes that occur in the system. Both models use Arrhenius expressions to account for the impact of temperature on the rate of change of activity of the biosensors. Note that the use of Arrhenius expressions for temperature dependencies is a semi-empirical approach, as the parameters estimated for the Arrhenius activation energies and pre-exponential factors do not necessarily represent the kinetic rate coefficients of the system; rather, they are lumped approximations reflecting changes in the reaction kinetic and mass transfer rates associated with the system, together with other thermally sensitive components in the biosensors.

The first-order and second-order dynamic models presented below are linear Ordinary Differential Equation (ODE) models for fixed temperature. The temperature dependence appears in the Arrhenius expressions that multiply activity terms in the right hand sides of the differential equations. In cases in which the temperature changes with time, the models can be used in a piecewise fashion. By assuming constant temperature between successive measurements of the storage temperature, the analytical solution to a particular linear ODE model can be used to relate the activity at the next time point to the predicted activity at the previous time point. The rate constants (represented by the Arrhenius expression(s)) over the time interval correspond to the temperature in the oven at the start of the time interval. In this way, dynamic sensor-response trajectories can be predicted for each experimental data set

(i.e., Data Set A with four storage temperature trajectories and Data Set B with three storage temperature trajectories).

2.2.4 First-order dynamic model

The preliminary model describing the change of biosensor activity over time uses a first-order dynamic model with Arrhenius temperature dependence for the rate constant:

$$\frac{dI_1}{dt} = -k_1 \cdot I_1 \tag{2}$$

where I_1 is the sensor response to the analyte in a liquid control sample; t is the sensor age; and k_1 is a lumped rate coefficient that has an Arrhenius temperature dependency of the form described in equation (1). Units for the parameters discussed in this work have been omitted to maintain confidentiality. Integration of equation (2), assuming constant temperature over a time interval of duration t, yields equation (3):

$$I_1 = I_{1_0} \cdot e^{-k_1 \cdot t} \tag{3}$$

where I_{1_0} is the response of the biosensor to the control fluid at the start of the interval, prior to the thermal exposure occurring over the interval. Equation (3) indicates that the biosensor activity is expected to follow an exponential decay trend. The parameters in this model were estimated using nonlinear least squares regression on the observations from data sets A and B.

2.2.5 Second-order dynamic model

In the second-order model, the aging behaviour of the biosensor is approximated using a two-step process between three states:

$$A \underset{k_{1\,rev}}{\overset{k_{1\,fwd}}{\Longleftrightarrow}} B \overset{k_{2\,fwd}}{\to} C \tag{4}$$

18

In the first step, the thermally-sensitive components of the biosensor in their native state A transition reversibly to an inactive state, labeled as B. In the second step, components in state B transition irreversibly to an inactive state C. In this scheme, it is assumed that biosensor components in state A function sufficiently well for the biosensor to respond to the presence of analyte as they would prior to aging. *B* and *C* represent states where the components of the biosensor no longer generate a response to the analyte of interest, or where the form of the response generated by the biosensor has changed so significantly that the algorithm for calculating analyte concentration is no longer appropriate. State B represents a reversibly modified state, whereas state C represents a terminal modified state. Note that this simple dynamic scheme is a lumped approximation to complex thermal aging interactions resulting from changes in components such as reaction kinetics and mass-transfer behaviour within the biosensor. The two-step aging mechanism in equation (4) is a simple way to account for complex temperature-dependent processes involving equilibration, changes in sensor responsiveness and long-term reductions in sensor activity. Similar kinetic aging models for use in accelerated testing have been used to describe changes in optical fiber systems [2.20].

In practice, the extent to which sensor performance has changed is determined by comparing the signal that it generates in response to a known standard. This signal is compared to the mean signal that was generated by sensors from the same lot, in response to the same known standard, prior to incubation and/or aging. Assuming that the rate of change for each transition in equation (4) follows first-order kinetics, the dynamic behaviour of the system can be summarized by two differential equations:

$$\frac{dI_A}{dt} = k_{1,rev}I_B - k_{1,fwd}I_A \tag{5}$$

$$\frac{dI_B}{dt} = k_{1,fwd}I_A - k_{1,rev}I_B - k_{2,fwd}I_B \tag{6}$$

where: I_A is the biosensor response to the analyte in a control sample, I_B is the hypothetical response that could be generated from component B if it were to revert back to A, and $k_{1,fwd}$, $k_{2,fwd}$, and $k_{1,rev}$ are rate coefficients. Using Arrhenius expressions to describe the temperature dependence of the transitions in equation (4) gives:

$$k_{1,fwd} = k_{1,fwd\_ref} \cdot e^{\left(\frac{-E_{k1,fwd}}{R}\left(\frac{1}{T}-\frac{1}{T_{ref}}\right)\right)} \tag{7}$$

$$k_{1,rev} = k_{1,rev\_ref} \cdot e^{\left(\frac{-E_{k1,rev}}{R}\left(\frac{1}{T}-\frac{1}{T_{ref}}\right)\right)} \tag{8}$$

$$k_{2,fwd} = k_{2,fwd\_ref} \cdot e^{\left(\frac{-E_{k2,fwd}}{R}\left(\frac{1}{T}-\frac{1}{T_{ref}}\right)\right)} \tag{9}$$

Where $E_{k_{1,fwd}}$, $E_{k_{1,rev}}$ and $E_{k_{2,fwd}}$ are lumped activation energies, T is the absolute temperature, and k_{1,fwd_ref}, k_{1,rev_ref} and k_{2,fwd_ref} are the rate coefficients at the reference temperature T_{ref}.

Equations (5) and (6) were solved analytically for I_A and I_B using the Maple™ symbolic mathematics software. An analytical solution exists for this model, which is a linear time-invariant system of ordinary differential equations under the assumption of piecewise constant temperature. When performing this integration over the first time interval, I_A is assumed equal to the mean time-zero biosensor reading obtained from un-aged sensors and that I_B is initially zero. For subsequent time intervals, the predicted values of I_A and I_B from the previous interval are used as initial values. A simplification is made to reduce the number of parameters requiring estimation, using an equilibrium constant (K_{eq}), which is

defined to relate the forward and reverse rates of the reversible reaction between species A

and B, as shown in equation (10):

$$K_{eq} = \frac{k_{1,rev}}{k_{1,fwd}} = \frac{k_{1,rev\_ref} \cdot e^{\left(\frac{-E_{k1,rev}}{R}\left(\frac{1}{T} - \frac{1}{T_{ref}}\right)\right)}}{k_{1,fwd\_ref} \cdot e^{\left(\frac{-E_{k1,fwd}}{R}\left(\frac{1}{T} - \frac{1}{T_{ref}}\right)\right)}} \qquad (10)$$

From equation (**10**), if $E_{k_{1,fwd}}$ and $E_{k_{1,rev}}$ are assumed to be equal, then the following

expressions can be derived:

$$K_{eq} = \frac{k_{1,rev\_ref}}{k_{1,fwd\_ref}} \qquad (11)$$

$$k_{1,rev} = k_{1,fwd\_ref} \cdot e^{\left(\frac{-E_{k1,fwd}}{R}\left(\frac{1}{T} - \frac{1}{T_{ref}}\right)\right)} \cdot K_{eq} \qquad (12)$$

This simplification is appropriate because parameter estimation using the full model

in equations (6) through (9) resulted in very similar values for the estimates of $E_{k_{1,fwd}}$ and

$E_{k_{1,rev}}$.

The use of equation (12) instead of equation (8) reduces the number of model

parameters from six to five. The resulting model solution equations are provided in Appendix

A.

2.2.6 Parameter estimation

The parameters in the first- and second-order dynamic models were estimated using

an ordinary least squares approach, applied to the results from Data Sets A and B. As noted

earlier, the time-varying temperature trajectory was accounted for by assuming that the

temperature was piecewise constant over each sampling interval. The analytical solutions to

the differential equation models, for a fixed temperature, were then used to propagate the predicted activity of the sensor forward one time step. This solution process was repeated recursively to obtain the predicted biosensor activity trajectories, which were used to generate the residuals for the least squares objective function. The optimization was performed using a generalized reduced gradient algorithm [2.21]. The initial parameter estimates were varied in a grid pattern and multiple optimizations were performed. The best solution, in terms of SSE minimization, was then selected from the results of these optimizations and the parameter estimates associated with this solution were used to predict responses from Data Set C.

2.3 *Results and Discussion*
2.3.1 **Experimental data**

Results from Data Set A (Figure 2.2), Data Set B (Figure 2.3) and Data Set C (Figure 2.4) demonstrate that under thermal stress conditions, the biosensor response to the liquid control sample diminishes over time. This trend is temperature-dependent, with biosensors stored at higher temperatures exhibiting a greater reduction in response. Note that the region of Figure 2.4 between time 0.04 and 0.08, corresponding to Data Set C lowest temperature, shows no appreciable shift in the mean biosensor response. These results from Data Set C show that the stability of the biosensor can be maintained effectively through storage at the lowest temperature. The Data Set A storage temperature fluctuations provide a "worst case scenario" test for storage (Figure 2.5), with occasional abrupt shifts in temperature, and considerable variability. Conversely, the oven temperatures were not varied much around the storage temperatures during the experiments in Data Set B (trajectory not shown). Note that the large and sustained temperature deviations in Data Set A could be a significant source of

22

error when developing models to describe sensor stability, if isothermal operation was assumed. Additional figures showing box plots for each event and storage condition in Data Sets A and B are included in Appendix E.
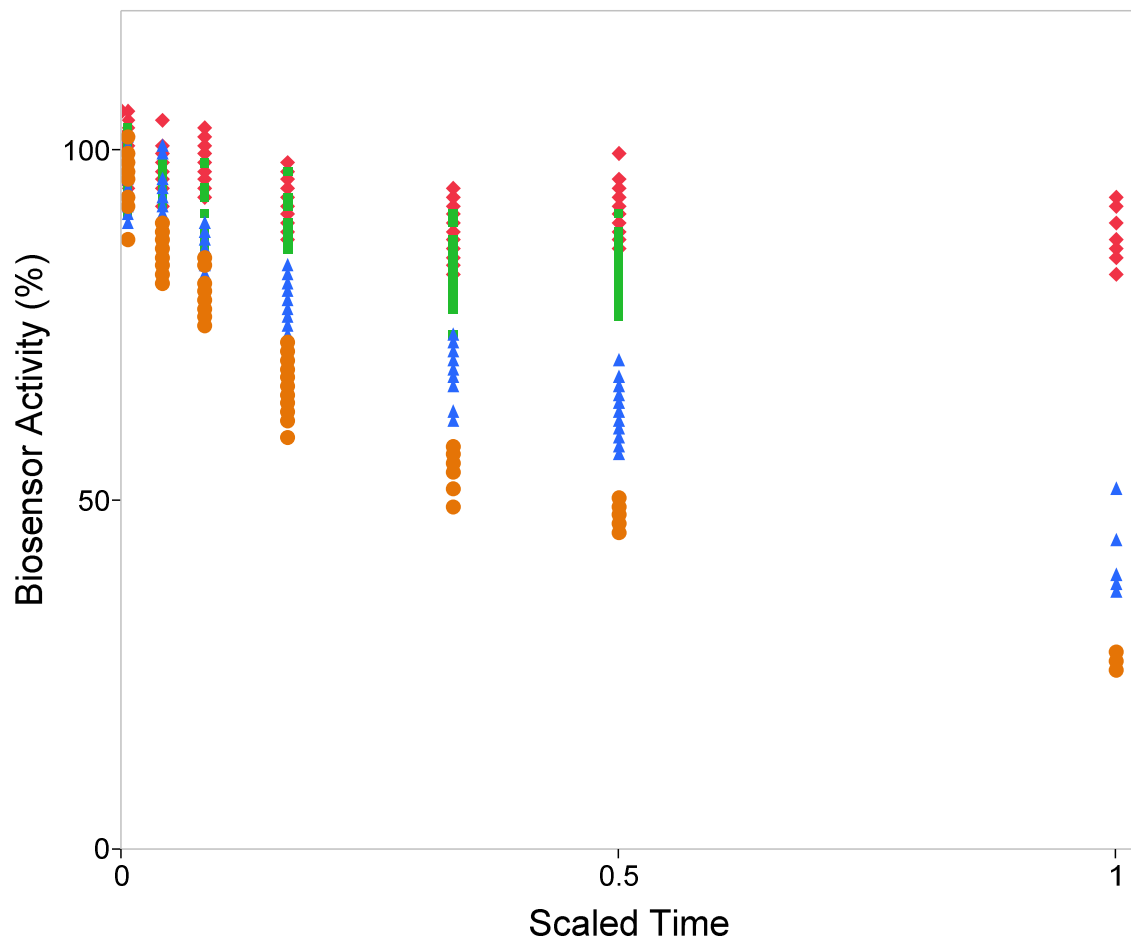
Figure 2.2: Data Set A - Biosensor response (% of initial activity) versus time for biosensors tested after storage at four different conditions (◆■▲●) of increasing temperature. Storage Condition I (◆) corresponds to the lowest temperatures and Storage Condition IV (●) corresponds to the highest temperatures tested. The time axis has been recoded as a fraction of the total duration of the Data Set A experiment.
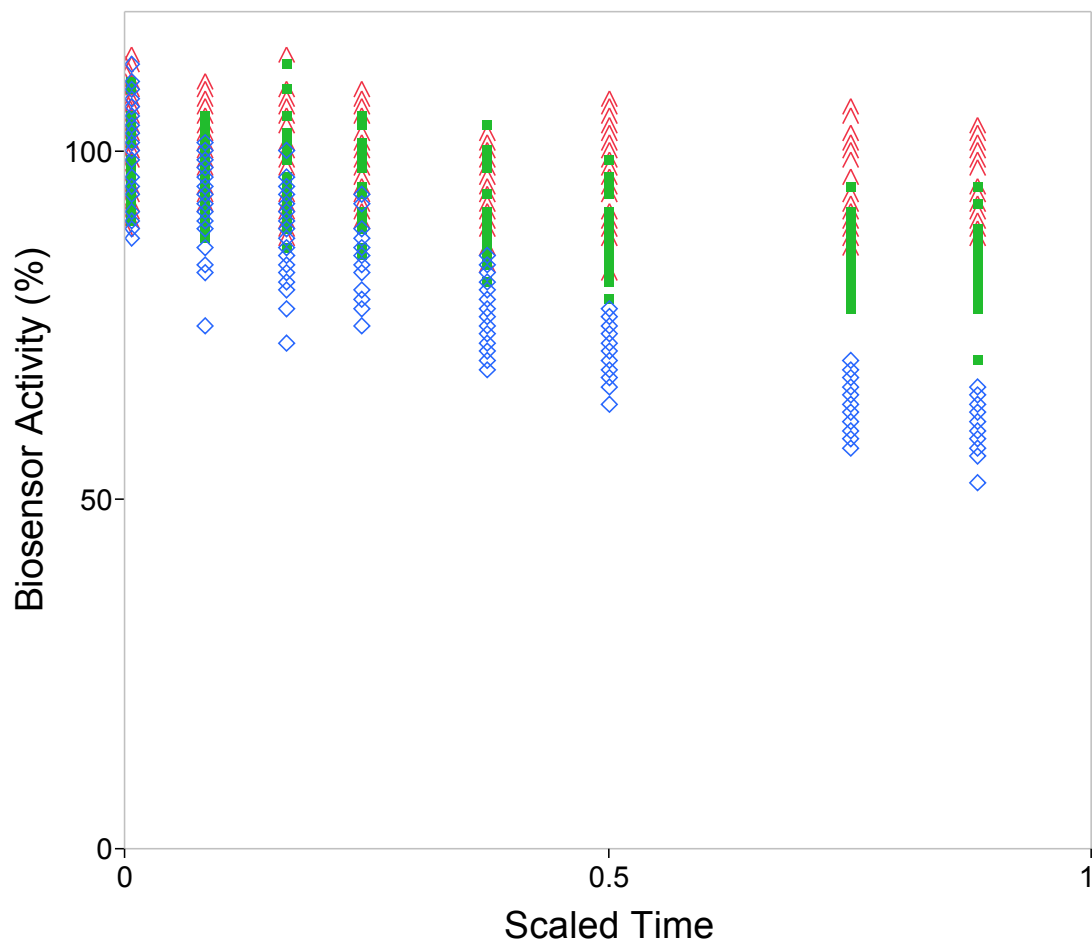
Figure 2.3: Data Set B - Biosensor response (% of initial activity) versus time for biosensors tested after storage at three different conditions (▲■◇) of increasing temperature. Storage Condition i (▲) corresponds to the lowest temperatures and Storage Condition iii (◇) corresponds to the highest temperatures tested. The time axis has been recoded as a fraction of the total duration of the Data Set A experiment.
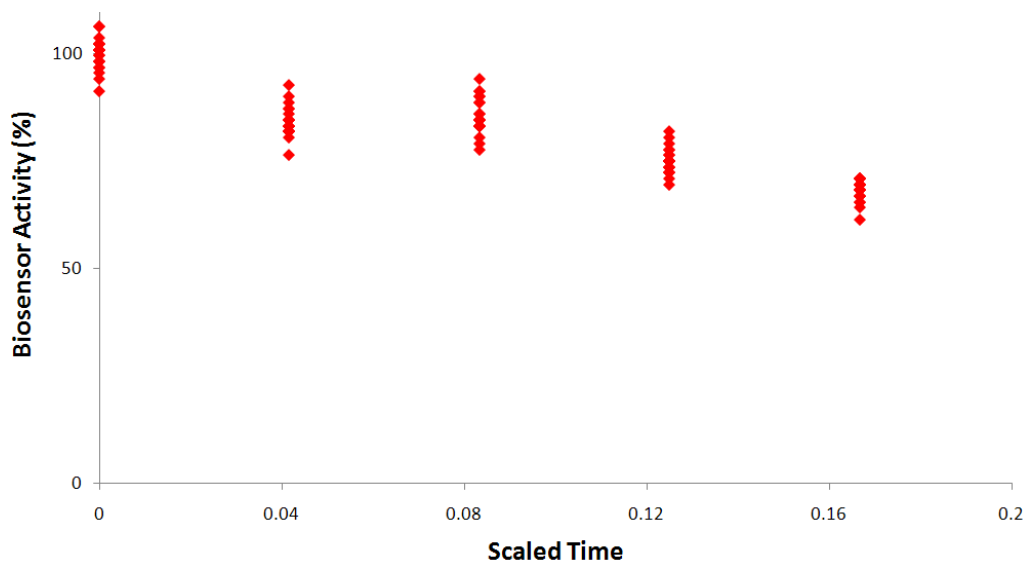
Figure 2.4: Data Set C - Effect of the non-constant storage conditions shown in Figure 2.1 on biosensor response over time. The time axis has been recoded as a fraction of the total duration of the Data Set A experiment.
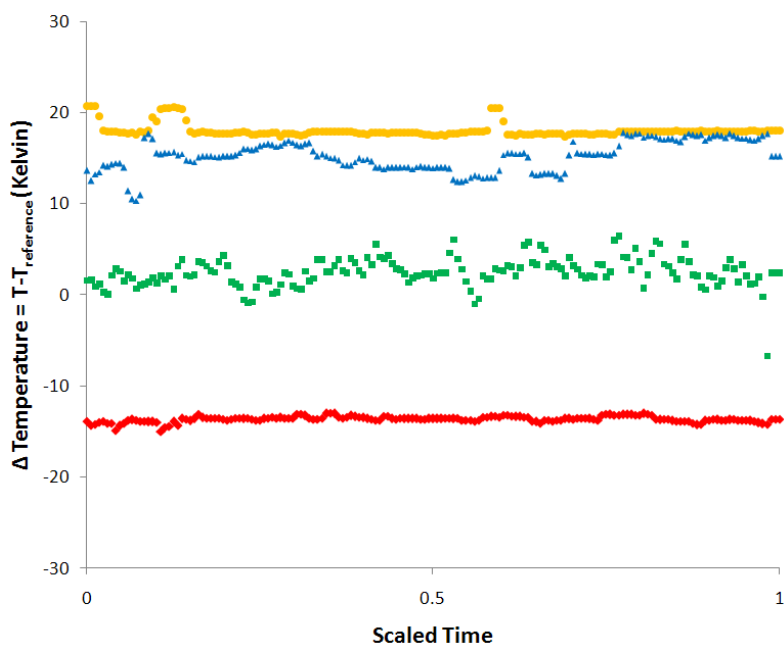
Figure 2.5: Temperature profiles recorded during storage of Data Set A biosensors. The data markers for each storage condition profile are as follows: Storage Condition I (◆), Storage Condition II (■), Storage Condition III (▲), Storage Condition IV (●). The time axis has been recoded as a fraction of the total duration of the Data Set A experiment.

25

2.3.2 Model fitting

To visually compare the modeling approaches from chapters 2.2.4 and 2.2.5, the fits of the first- and second-order dynamic models to the results from Data Set A were plotted for storage conditions III and IV (Figures 2.6 and 2.7).
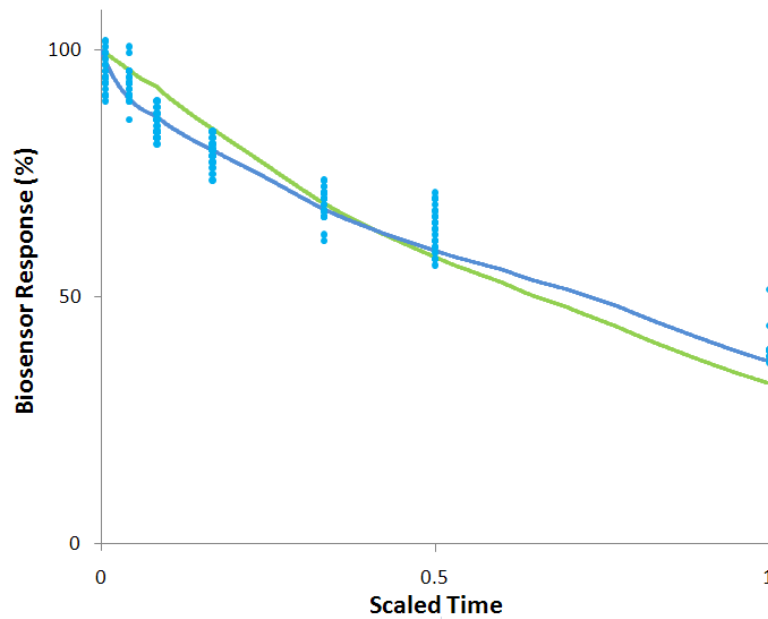
Figure 2.6: Biosensor response versus time at Storage Condition III (●), with predictions from both the first-order (—) and second-order (—) dynamic models plotted for comparison. The time axis has been recoded as a fraction of the total duration of the Data Set A experiment.
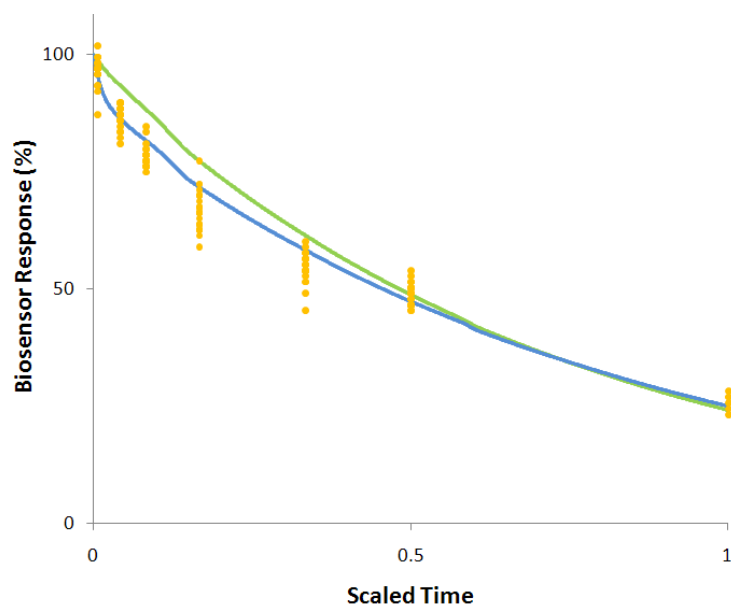
Figure 2.7: Biosensor response versus time at Storage Condition IV (●), with predictions from both the first-order (—) and second-order (—) dynamic models plotted for comparison. The time axis has been recoded as a fraction of the total duration of the Data Set A experiment.

The predictions from the second-order dynamic model track the trend in the data much more closely than the first-order model predictions, particularly for times less than 0.50. The plots in figures 2.6 and 2.7 show that the decay trend explained by the first-order model corresponds to the long-time changes in activity, rather than the earlier shift. This provides additional evidence that there are multiple thermally-sensitive behaviours present in the data, working at several time scales.

The second-order model was formulated using a combination of physical insight and by noting the inadequacies of the first-order model fit relative to the observed trajectories. The activity trajectories appear to exhibit multiple time scales suggesting more rapidly changing and less rapidly changing contributions to the biosensor stability. Alternative second-order dynamic models were also investigated (Appendix D). A second-order

dynamic model without reversible kinetics failed to capture more of the observed behaviour relative to the first-order dynamic model fit, further motivating the consideration of a reversible reaction element in the model. Of the second-order dynamic models investigated, the model form described by equation 4 provided the best fit to Data Sets A and B. To assess the improvement in fit resulting from the second-order model chosen, adjusted R^2 values and mean-squared error were calculated for each of the two models (Table 2.1).

Table 2.1 Diagnostic statistics for each model fit to Data Sets A and B

Nominal Storage Temperature	1st order dynamic model	2nd order dynamic model
MSE	2.69×10^{-5}	2.13×10^{-5}
Adjusted R^2	0.796	0.839

The second-order dynamic model achieves a better fit to the experimental data, in terms of the statistics in Table 2.1 and by comparison of predicted trajectories versus the observations (Figures 2.6 and 2.7). For the special case where parameters K_{eq} and k_{2,fwd_ref} are both set to zero, the proposed second-order dynamic model reduces to the first-order dynamic model. This means that the first-order dynamic model is nested within the proposed second-order dynamic model and that a mean square ratio test can be performed to determine whether the second-order dynamic model gives a significantly better fit to the data. For this case, the test statistic takes the following form (equation 13):

$$F = \frac{\left(\dfrac{SSE_1 - SSE_2}{p_2 - p_1} \right)}{\left(\dfrac{SSE_2}{n - p_2} \right)} \tag{13}$$

28

where $SSE_1=0.0381$ and $SSE_2=0.0302$ are the sums of squared residuals for the first- and second-order models respectively, $p_1=2$ is the number of parameters for the first-order model, $p_2=5$ is the number of parameters in the second-order model, and $n=1419$ is the total number of observations from Data Sets A and B that were used to fit the parameters. The test compares the mean square difference in the residual error between the full model and the model with the smaller number of terms, to the mean square error of the larger model. Under the null hypothesis, it is assumed that the test statistic follows an F distribution with $(p_2 - p_1, n - p_2)$ degrees of freedom. The null hypothesis corresponds to the case in which the additional terms in the second-order dynamic model do not explain a statistically significant amount of variation, implying that the second-order dynamic model does not provide a significantly better fit than the first-order dynamic model. From the data in Data Sets A and B, this null hypothesis can be rejected at the 95% confidence level, because the resulting large value of the test statistic (F=123) is much higher than the critical value $F_{(0.05,3,1414)} = 2.61$ of the F distribution. This statistical test provides additional confirmation that the second-order dynamic model provides a significantly better fit of Data Sets A and B than the first-order dynamic model.

2.3.3   Parameter confidence intervals

Approximate confidence intervals for the parameter estimates were obtained by linearizing the model around the optimal parameter estimates [2.22]. The approximate confidence intervals are described by (equation 14):

$$\left[\hat{\beta}_i - t_{\left(v,\frac{\alpha}{2}\right)} \cdot s_{\hat{\beta}_i}, \hat{\beta}_i + t_{\left(v,\frac{\alpha}{2}\right)} \cdot s_{\hat{\beta}_i} \right]$$

(14)

where $\hat{\beta}_i$ is the estimate for the ith parameter, $s_{\hat{\beta}_i}$ is the standard deviation of the ith parameter estimate obtained from the approximate covariance matrix provided by the linearization. $t_{\left(v,\frac{\alpha}{2}\right)}$ is the value of the t-distribution with v degrees of freedom at significance level $\left(\frac{\alpha}{2}\right)$ (a significance level of $\alpha = 0.05$, corresponds to 95% confidence intervals). This approach produces symmetrical confidence intervals, which may be invalid if the influence of the parameters on the model predictions is highly nonlinear [2.22]. $s_{\hat{\beta}_i}$ was computed using a pooled estimate of the pure error variance, generated from the 10 to 24 replicate data points at each testing event, assuming that the noise variance is constant. The resulting confidence intervals for the parameters are shown in Table 2.2. For all five parameter estimates, the confidence intervals do not include zero, indicating that the parameter estimates are significantly different from zero at the 95% confidence level.

Table 2.2 Parameter confidence intervals for the second-order dynamic model

Parameter	Parameter Value	95% confidence interval
k_{1,fwd_ref}	1.608×10^{-2}	$[8.800 \times 10^{-4}, 3.128 \times 10^{-2}]$
k_{2,fwd_ref}	2.275×10^{-2}	$[4.150 \times 10^{-3}, 4.135 \times 10^{-2}]$
K_{eq}	6.849×10^{0}	$[2.215 \times 10^{0}, 1.148 \times 10^{1}]$
$E_{k_{1,fwd}}$	8.105×10^{4}	$[5.257 \times 10^{4}, 1.095 \times 10^{5}]$
$E_{k_{2,fwd}}$	1.155×10^{5}	$[6.763 \times 10^{4}, 1.634 \times 10^{5}]$

2.3.4 Model Validation using Data Set C

In order to further assess the predictive ability of the estimated models, the first- and second-order models with parameter estimates from Data Sets A and B were used to predict the Data Set C outcomes. The experimental data and the predictions from the first-order and second-order dynamic models are shown in Figure 2.8.
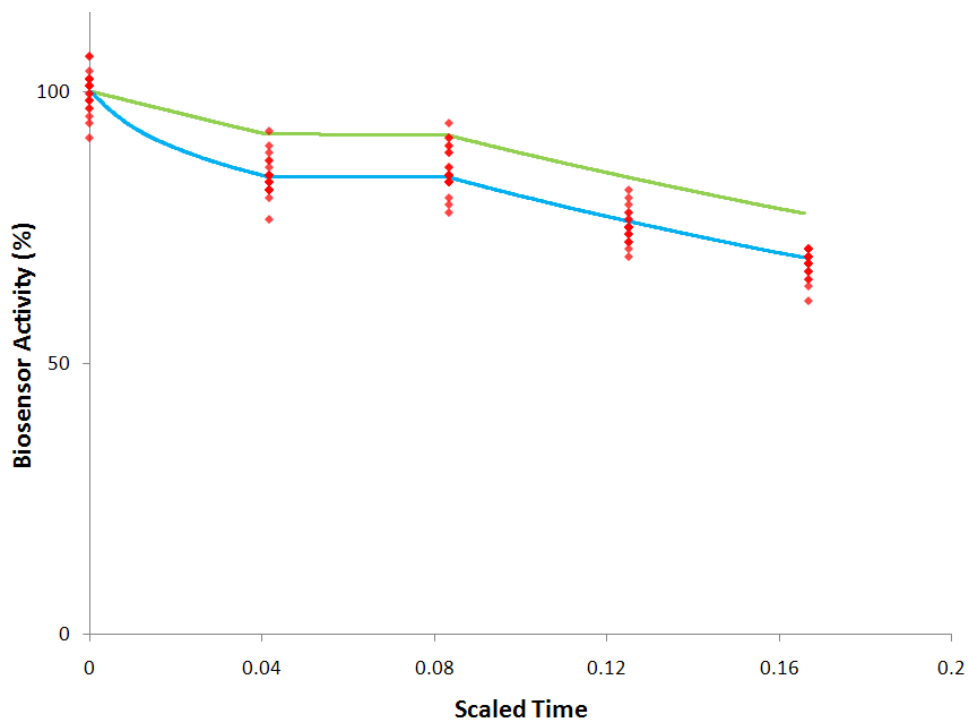
Figure 2.8: Effect of the non-constant storage conditions shown in Figure 2.1 on biosensor responses (◆) over time. First-order (—) and second-order (—) model predictions are plotted for comparison. The time axis has been recoded as a fraction of the total duration of the Data Set A experiment.

The sensor responses predicted by the second-order dynamic model agree very well with the experimental results from Data Set C, whereas the predictions from the first-order dynamic model are not accurate and show a sustained prediction bias. The duration of Data Set C is roughly 20% of the duration of Data Set A, so the validation test is focused on short-

and medium-term time behaviour and confirms that the second-order model is suitable for practical use.

The predictive ability of the second-order dynamic model makes it a powerful tool for the design and interpretation of accelerated testing experiments. It may also be useful for investigating opportunities for product improvements. Finally, the model is useful for simulating the response of the biosensors to potential, or actual, storage and shipping scenarios involving temperature variations.

2.3.5 Mean Kinetic Temperature

The MKT is defined by both the United States Food and Drug Administration (USFDA) [2.14] and Health Canada [2.15] as :

"A single derived temperature that, if maintained over a defined period of time, affords the same thermal challenge to a drug substance or drug product as would be experienced over a range of both higher and lower temperatures for an equivalent defined period. The mean kinetic temperature is higher than the arithmetic mean temperature and takes into account the Arrhenius equation."

The FDA recommends computing the MKT using the following equation [2.14]:

$$MKT = \frac{\dfrac{E_a}{R}}{-\ln\left(\dfrac{e^{\frac{-Ea}{RT_1}} + e^{\frac{-Ea}{RT_2}} + \cdots + e^{\frac{-Ea}{RT_n}}}{n}\right)} \tag{15}$$

where n is the number of equally-spaced temperature readings over the storage period and T_i is the absolute temperature during the ith time interval. Note that equation (15) was derived assuming a first-order dynamic model for drug potency. We propose that the concept of MKT could be extended to and used for analyzing lifetime stability changes in systems

32

exhibiting higher-order dynamics. For example, the second-order dynamic model in this article can be used to solve for the constant temperature that would yield the same level of biosensor activity loss that was encountered in Data Set C. This procedure involves using the second-order model and the temperature time trajectory to predict the final activity value, and then setting the storage duration and final biosensor activity value to solve the implicit algebraic equation (see the appendix) for the unknown MKT. Since the system is modeled by a complex, highly nonlinear equation, solving for the temperature analytically is much more difficult than computing the traditional MKT from equation (15).   Formally, if $\theta(t_i, t_{i-1}, T_{i-1})x_{i-1}$ represents the solution to the differential equation model with constant temperature T_{i-1}, and the starting activity is x_{i-1} at time t_{i-1}, then the final activity value is:

$$\theta(t_n, t_{n-1}, T_{n-1})\theta(t_{n-1}, t_{n-2}, T_{n-2})\cdots\theta(t_1, t_0, T_0)x_0 \qquad (16)$$

where x_0 is the initial activity, and n is the number of temperature intervals. The resulting expression for the MKT based on the higher-order model is the solution to:

$$\theta(t_f, t_0, MKT)x_0 = \theta(t_n, t_{n-1}, T_{n-1})\theta(t_{n-1}, t_{n-2}, T_{n-2})\cdots\theta(t_1, t_0, T_0)x_0 \qquad (17)$$

The multiplicative form of the solution to the differential equation comes from the fact that it is a linear time-invariant differential equation for fixed temperature. Equation (15) can be derived using a similar approach, in which $\theta(t_i, t_{i-1}, T_{i-1})x_{i-1} = e^{-k(t_i - t_{i-1})}x_{i-1}$, where $k = f(T_{i-1})$ is the Arrhenius expression for the rate at temperature T_{i-1}.

The MKT calculation was set up as an optimization problem and solved using a generalized reduced gradient nonlinear optimizer [2.21] to minimize the difference between

the left and right hand sides of equation A1 with the set final activity and duration. The resulting MKT value that would yield the measured biosensor activity at the end of the storage period for Data Set C is plotted in Figure 2.9. Also shown in the figure is the traditional MKT for computed using equation (15), which assumes a first-order process for biosensor stability. Note that the estimated parameter value $E_a = 69161$ obtained by fitting the first-order model to Data Sets A and B was used in this calculation.
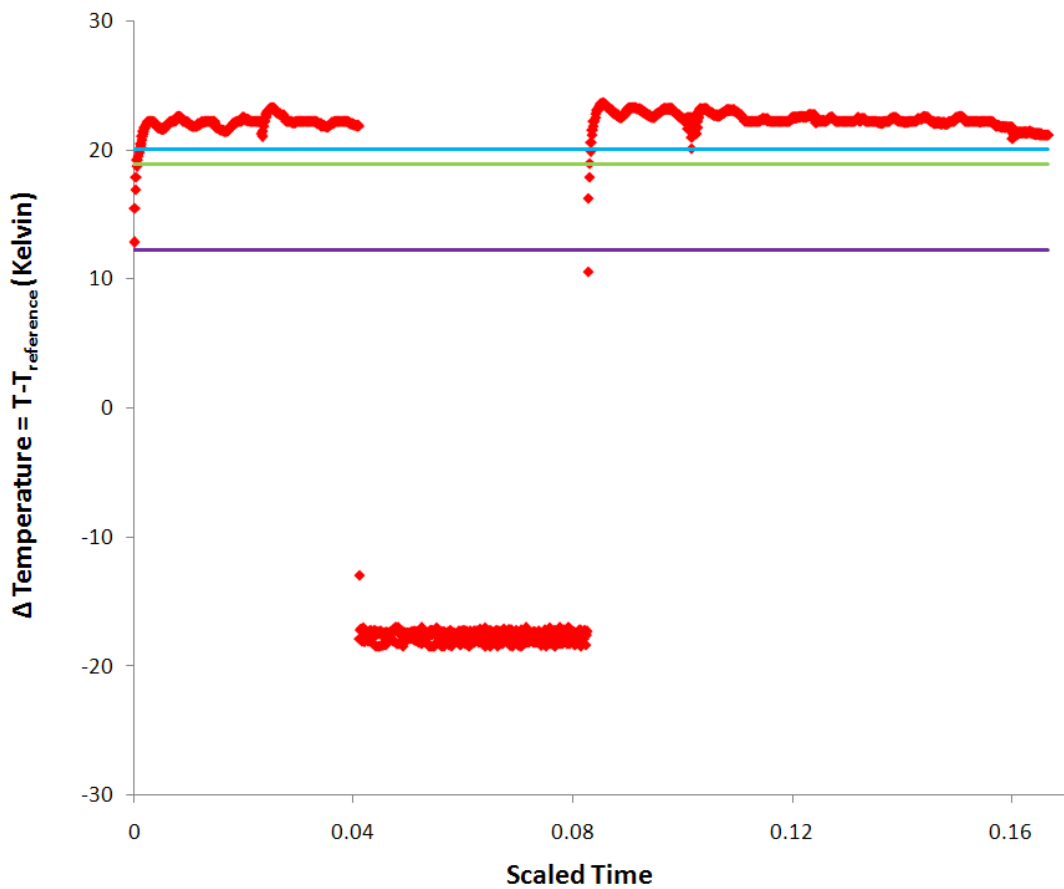
Figure 2.9: Data Set C temperature profile (◆) along with the calculated first-order MKT (—), second-order MKT (—) and average temperature (—). The time axis has been recoded as a fraction of the total duration of the Data Set A experiment.

From Figure 2.9, the MKT calculated using the second-order dynamic model is higher than the MKT calculated from equation (15), and both MKT estimates are higher than the arithmetic average temperature from Data Set C. The MKT values estimated using the first- and second-order models emphasize the pronounced effect that storage at high temperatures has on the stability of the sensor. The fact that the MKT based on the second-order model is higher than that computed using the first-order model reflects the under-prediction of the changes that were observed from the estimated first-order model. These results have implications for shelf-life monitoring of enzyme-based biosensor products, as they indicate that the calculation of the MKT based on the traditional first-order aging model for pharmaceutical applications may not fully describe biosensors that demonstrate higher-order aging behaviour. Instead, models that account for higher-order dynamics of biosensor aging behaviour should be used to solve for MKT, to establish appropriate expiration and shelf-life guidelines. A final observation is that the first-order model tends to under-predict the change in activity, compared to the second-order model. This has implications for designing accurate accelerated testing protocols, to avoid situations in which more pronounced aging occurs because of aggressive accelerated testing based on less accurate models.

2.4   *Conclusions*

A semi-empirical second-order dynamic model has been proposed to predict changes in biosensor activity under varying thermal storage conditions. The proposed second-order dynamic model shows improved fit (in terms MSE, and adjusted R^2 statistics) to estimation datasets, relative to a first-order dynamic model. The first- and second-order models are nested, and a significance test further confirms that the additional terms in the second-order

35

model are accounting for significant variation. The parameters are statistically significant from zero at the 95% confidence level based on individual approximate confidence intervals. Finally, the second-order model is seen to have good predictive ability for a validation dataset not used for estimation, compared to the first-order model.

The second-order model provides good predictions of biosensor response to dynamic temperature excursions. These results indicate that, for the biosensor product line of interest, a second-order dynamic model provides a better description of the thermally-driven aging pathways involved than does a traditional first-order model. The second-order dynamic model has potential applications for shelf-life predictions, for the design and interpretation of accelerated testing experiments and for investigating opportunities for product improvement. Finally, the results show that the traditional form of the MKT calculation should not be used for the biosensor investigated. Rather, calculation of MKT using the proposed second-order dynamic model provides more accurate results for the development of product storage guidelines. The definition of the MKT is extended to second- (and higher-) order dynamic models, and the computation of the MKT is demonstrated.

2.5 *Role of the funding source*

2.6   *References (Chapter 2)*

[2.1] K. Lewandrowski, Point-of-Care Testing: An Overview and a Look to the Future (Circa 2009, United States), Clin. Lab. Med. 29 (2009) 421-432.

[2.2] P. d'Orazio, Biosensors in clinical chemistry, Clin. Chim. Acta 334 (2003) 41-69.

[2.3] T. Schulmeister and D. Pfeiffer, Mathematical modeling of amperometric enzyme electrodes with perforated membranes, Biosens. Bioelectron. 8 (1993) 75-79.

[2.4] T. Rinken and T. Tenno, Dynamic model amperometric biosensors. Characterisation of glucose biosensor output, Biosens. Bioelectron. 16 (2001) 53-59.

[2.5] R. Krishnan, P. Atanasov and E. Wilkins, Mathematical modeling of an aperometric enzyme electrode based on a porous matrix of Stöber glass beads, Biosens. Bioelectron. 11 (1996) 811-822.

[2.6] P.N. Bartlett and K.F.E. Pratt, Modeling of processes in enzyme electrodes, Biosens. Bioelectron. 8 (1993) 451-462.

[2.7] P. Boeker, O. Wallenfang and G. Horner, Mechanistic model of diffusion and reaction in thin sensor layers – the DIRMAS model, Sens. Actuators B 83 (2002) 202-208.

[2.8] F. Thalmayr and G. Fischerauer, Sensor signal processing for gravimetric chemical sensors based on a state-space model, Sens. Actuators B 144 (2010) 27-36.

[2.9] G. Fischerauer and F. Dickert, An analytical model of the dynamic response of mass-sensitive chemical sensors, Sens. Actuators B 123 (2007) 993-1001.

[2.10] T.D. Gibson, J.N. Hulbert, S.M. Parker, J.R. Woodward and I.J. Higgins, Extended shelf life of enzyme-based biosensors using a novel stabilization system, Biosens. Bioelectron. 7 (1992) 701-708.

[2.11] N.A. Chaniotakis, Enzyme stabilization strategies based on electrolytes and polyelectrolytes for biosensor applications, Anal. Bioanal. Chem. 378 (2004) 89-95.

[2.12] S. Cosnier, Biomolecule immobilization on electrode surfaces by entrapment or attachment to electrochemically polymerized films. A review, Biosens. Bioelectron. 14 (1999) 443-456.

[2.13] J.T. Carstensen, M. Franchini and K. Ertel, Statistical approaches to stability protocol design, J. Pharma. Sci. 81 (1992) 303-308.

[2.14] U.S. Food and Drug Administration, Guidance for industry: Q1A(R2) Stability testing of new drug substances and products, . U.S. Department of Health and Human Services;

Food and Drug Administration; Center for Drug Evaluation and Research (CDER); Center for Biologics Evaluation and Research (CBER). (2003). Accessed Online: December, 2010. Web Address: http://www.fda.gov/RegulatoryInformation/Guidances/ucm128179.htm

[2.15] Health Canada, Adoption of ICH Guidance: Stability Testing of New Drug Substances and Products: ICH Topic Q1A(R2), Bureau of Pharmaceutical Sciences; Therapeutic Products Directorate; Health Canada. (2003). Accessed Online: December, 2010. Web Address: http://www.hc-sc.gc.ca/dhp-mps/prodpharma/applic-demande/guide-ld/ich/qual/q1a(r2)-eng.php

[2.16] D.G. Watts, Estimating parameters in nonlinear rate equations, Can. J. Chem. Eng. 72 (1994) 701-710.

[2.17] B. Kommanaboyina and C.T. Rhodes, Effects of temperature excursions on mean kinetic temperature and shelf life, Drug Dev. Ind. Pharm. 25 (1999) 1301-1306.

[2.18] K. McAteer, C.E. Simpson, T.D. Gibson, S. Gueguen, M. Boujtita and N. El Murr, Proposed model for shelf-life prediction of stabilized commercial enzyme-based systems and biosensors, J. Mol. Catal. B: Enzym. 7 (1999) 47-56.

[2.19] C.-X. Liu, L.-Y. Jiang, H. Wang, Z.-H. Guo and X.-X. Cai, A novel disposable amperometric biosensor based on trienzyme electrode for the determination of total creatine kinase, Sens. Actuators B, 122 (2007) 295-300.

[2.20] M.J. LuValle, An approximate kinetic theory for accelerated testing, Inst. Ind. Eng. Trans. 31 (1999) 1147-1156.

[2.21] D. Fylstra, L. Lasdon, J. Watson and A. Waren, Design and use of the Microsoft excel solver. Interfaces 28 (1998) 29-55.

[2.22] D.M. Bates and D.G. Watts, Nonlinear regression and its applications, Wiley, New York, 1988.

Chapter 3: Modeling the Thermal Stability of a Diagnostic Assay

3.1 Introduction

To continuously improve the stability, accuracy, efficiency and overall quality of the diagnostic assay cartridges delivered to their customers, Abbott Point of Care (APOC) monitors product performance and attempts to identify areas in which improvements could be made. Recently, historical and experimental data for one of the APOC assays were analyzed to investigate methods for extending the shelf-life of the product beyond the current claims. This investigation provided an opportunity to build on experience from our previous modeling work (Chapter 2). Both this assay system and the assay system in Chapter 2 are used to quantify concentrations of specific analytes in patient blood samples.

The APOC i-STAT® diagnostics system consists of the i-STAT® handheld analyzer and individual, single-use diagnostics assay cartridges. Many of the cartridges contain multiple assays and test the concentrations of a panel of analytes in a patient blood sample using electrochemical sensors. A calibration package is also contained within the cartridge, and fluid from this package is analyzed prior to the blood sample from the patient. The calibration fluid contains known concentrations of analytes, and is used to generate reference or baseline values for comparison to the resulting response signals from the patient blood sample. The relationships between the true values of analyte concentrations in the blood sample and the electrical response signals generated by the sensors after exposure to both the calibration fluid and blood sample are contained within the equations and algorithms of the i-STAT® analyzer software. This software enables the concentration of specific analytes to be reported by the analyzer in a timely manner.

As described in Chapter 2, mathematical modeling plays a significant role in the design and implementation of sensor diagnostic systems. Calibration models are required to relate the electrical signal generated in the sensor's circuits to the concentrations that are measured [3.1-3.3]. The calculation of analytically useful information from the sensor response signals depends on the stability of the sensor system. Assumptions concerning sensor activity, reference standards, signal-to-noise ratio and signal gain must remain constant, or else changes in these factors over time must be accounted for in the modeling process. When the sensor system is exposed to stressful storage conditions, such as elevated temperature, the relationships between the electrical sensor response and the physical properties measured by the sensor may change [3.4,3.5]. These changes can cause the model equations, which are used for the calculation of analytical results, to require minor adjustments to their form or parameters, or can cause them to become completely invalid for the resulting altered system.

A stability model for the assay of interest may be useful for quantifying the underlying changes in sensor behaviour that occur due to thermal exposure. The model development process itself is also a valuable task to engage in, as it requires the investigation of the stability process and involves the identification of possible causes for the changes observed.

The stability of the assay of interest was investigated through modeling to describe the behaviour of the assay over its lifetime and to identify the areas where improvements to stability of the assay and/or its components can be made. A first-order dynamic model was fit to the long-term assay response data, collected from thermally stressed assay cartridges. An additional experimental program was designed and implemented for use in parameter

estimation. Model parameters were estimated from both the long-term assay response data and the new data set generated from the experimental program. Three additional experimental data sets were used for model validation. The resulting model indicates that the stability issue for the assay seems to be caused by changes over time in the analyte concentration of the calibration fluid packaged with the assay. Because the first-order model was able to predict the trends in the validation data, higher-order models were not required. Data discussed throughout this chapter have been coded to protect the intellectual property of APOC.

3.2   *Experimental Data*

Six experimental data sets were analyzed over the course of this modeling work. The results from five of the experimental programs had been collected prior to the initiation of this modeling work, and the sixth experimental program was designed and implemented during the project. Three of the initial experimental programs involved the incubation of whole cartridges at elevated temperatures. These experimental programs will be referred to as Experiments D, E and F for the remainder of this chapter. The temperatures used for experiments D, E and F spanned a similar range, and although there was some overlap, not all of the temperature levels tested were replicated in each experiment. The experimental testing plan for data sets D, E and F are included as Table B3 in Appendix B.

Experiment G involved the isolation of sensors from the rest of the cartridge components, and the storage of these sensors at elevated temperatures, independent of other components. Following the application of thermal stress to the sensors, cartridges were then assembled with new components, using the stressed sensors. This procedure allowed for conclusions to

be drawn concerning the thermal stability of the sensor itself. The experimental testing plan for data set G is included as Table B4 in Appendix B.

In experiment H, calibration fluid packages were stored at elevated temperatures, to determine the effect of thermal stress on the reference analyte levels within the calibration fluid. Concentrations of analyte present in the calibration packages after exposure to thermal stress were determined by testing the fluid with APOC assay cartridges that had been stored under the recommended conditions.

Finally, experiment I was designed and implemented to complement the results from experiment H. Experiment I, like experiment H, involved the incubation of calibration packages at elevated temperatures, and their subsequent testing using stable APOC assay cartridges. The temperatures used for experiment I differed from those used in experiment H, so that the combined results from the two experiments covered a large range of temperatures for estimating the kinetic parameters of the system. The testing plans associated with experimental data sets H and I are included as Table B5 in Appendix B.

3.3   *Preliminary Analysis of Prior Data*

Abbott's diagnostic assay cartridges are routinely used to test samples of known analyte concentration for quality monitoring. From historical data sets, it is apparent that the readings of these single-use cartridges begin to deviate from the assigned value of the control samples once they are well past the end of their useable lifetime. It was therefore of interest to APOC scientists to design experiments and track assay performance from the time of product manufacture, to the end of the cartridge lifetime, and to explore the effect of exposing the cartridge system to potential extremes in storage conditions. Results from the first round of experiments where cartridges were exposed to a variety of storage temperatures

were available at the onset of this work, from prior APOC studies. Figure 3.1 shows the behaviour of three representative sets of cartridges stored at a temperature above their specified storage temperature limit, and tested using aqueous samples of known, nominally equivalent analyte concentrations.
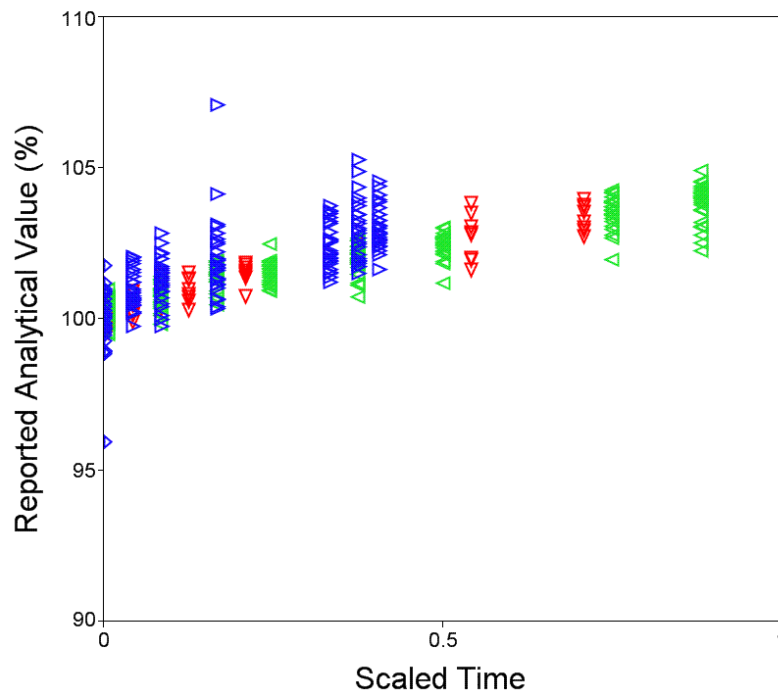
Figure 3.1: Estimate of analyte concentration from the assay of interest as a percentage of the initial value after storage at an elevated temperature, for Experiments D (◁), E(▷) and F(▽). The time axis has been recoded as a fraction of the longest duration for the experiments.

The reported analyte concentration from the assay for the control sample increases after exposure to elevated temperatures, as shown clearly from the results of experiments D and E.   The temperature effect increases in magnitude with the duration of exposure, and is likely related to the stability of one or more cartridge components. The initial experiments D, E and F that identified the stability behaviour shown in Figure 3.1 were followed by further experimentation (experiments G, H and I) to determine which cartridge components

contributed to the stability problem. The control sample used for testing is a fluid of known analyte concentration, and has been ruled out as the cause of the deviation. An additional figure showing box plots for test each event represented in Figure 3.1 (Data Sets D, E and F) is included in Appendix E.

In experiment G, the sensors were isolated and thermally stressed, separately from the remainder of the cartridge. The results from this experiment show that the stability issue is independent of sensor exposure (Figure 3.2), as indicated by the consistency of reported analytical assay values when the sensor was the only component exposed to elevated temperatures.
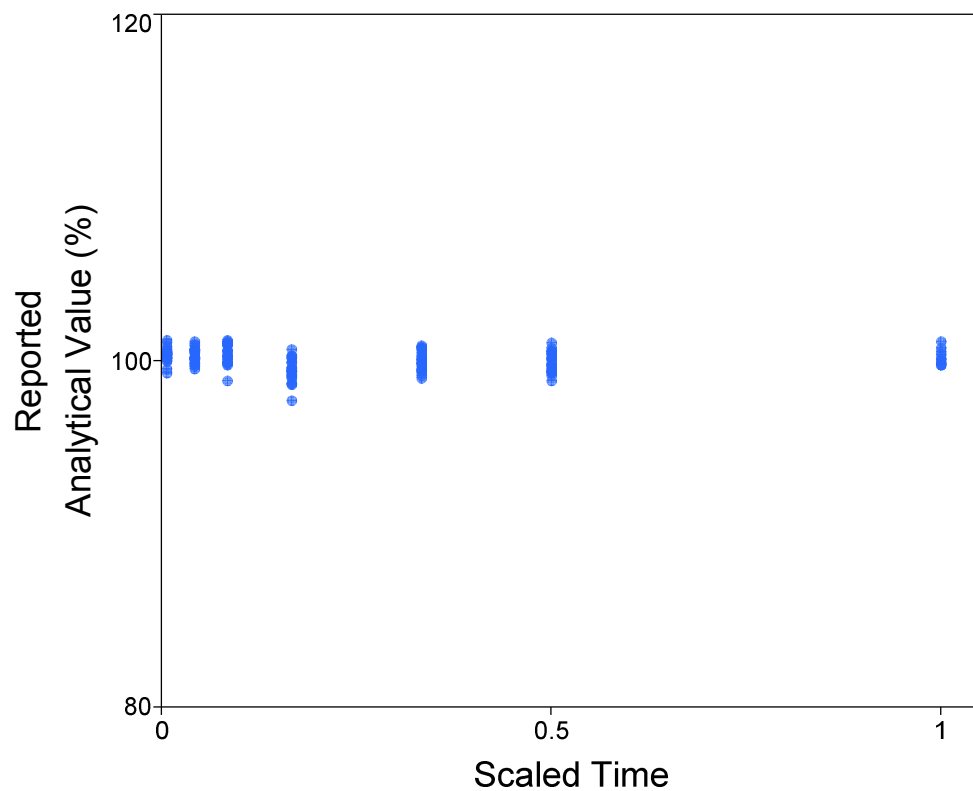
Figure 3.2: Assay response after sensor exposure to elevated temperatures. Other cartridge components were stored under normal conditions.

44

Next, APOC scientists investigated the stability of the analyte in the calibration package of the cartridge. This calibration package, included within each assay cartridge, contains chemical reference substances that may be susceptible to changes over time. The calibration fluid from the package makes contact with the sensor prior to the sample fluid which is to be analyzed. The calibration fluid provides a baseline sensor reading and has a known analyte composition, to which the sample signal is compared, so that it can be transformed into a measured concentration value. Experiment H, which involved subjecting calibration packages to thermal stress independently from other sensor components was carried out, and the results show that the level of analyte in the calibration fluid diminishes over time, with exposure to elevated temperatures (Figure 3.3). This effect is more pronounced after storage at higher temperatures.
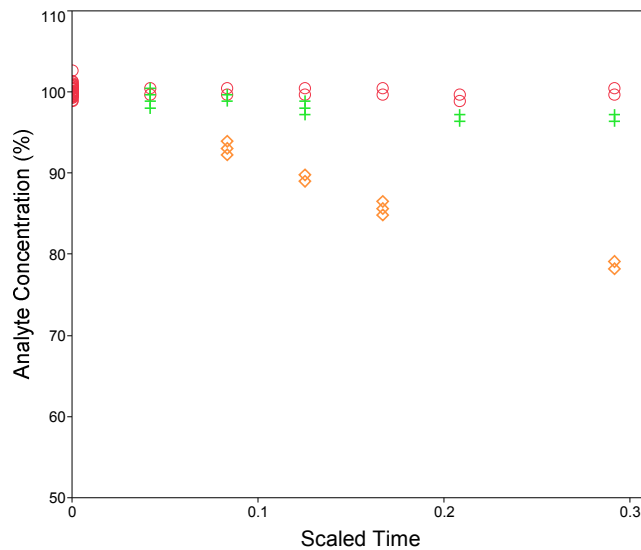
Figure 3.3: Results from calibration fluid packages stored at elevated temperatures and then tested using diagnostic cartridges stored under normal conditions. Analyte concentration is expressed as a percentage of the original analyte concentration in the calibration fluid. Storage condition 1 (O) corresponds to the lowest temperature level tested, whereas storage condition 3 (◇) corresponds to the highest temperature level tested. Note that some symbols are darker than others due to a higher density of data.

45

From experiments D through I, it was concluded that to improve assay performance beyond its currently specified limits for storage temperature and shelf-life, the research focus should be on thermal stability of the analyte in the calibration fluid package. The focus of our modeling work, therefore, is on the stability of the analyte within the calibration package system and the associated impact on assay results.

3.4   Experimental Design for Parameter Estimation

To develop a stability model of the analyte levels within the calibration package, additional experimental data for parameter estimation were collected. Experiment H (Figure 3.3) has a large gap between the temperatures for storage conditions 2 and 3, where more information would be useful. Experiment I was designed and implemented to help fill this gap in the available data and to extend the overall temperature range. In experiment I, calibration fluid packages were stored at two different temperatures (denoted conditions 2a and 4). Condition 2a had a temperature between those for conditions 2 and 3, and condition 4 used a temperature that was higher than that for condition 3. Experiment I also included calibration packages spiked with increased levels of other calibration fluid species, which had been identified as potential contributing factors to the stability of the analyte in the package. To test the calibration fluid, a sample was drawn from each individual calibration package and tested on normal APOC assay cartridges (cartridges that had not been exposed to elevated temperatures).

3.5   Data Analysis and Model Fit

The analyte concentration within the calibration fluid decreases over time, during exposure to elevated temperature. This behaviour could be caused by a variety of mechanisms, such as chemical transformations of the analyte, leakage of the analyte from the

package or absorption of the analyte into layers of the packaging material. As an initial exploration of these options, a model for a first-order, single-step reaction was fit to the data. The mechanism for the model used has the following structure:

$$A \xrightarrow{k_{1\,fwd}} B \tag{18}$$

where A represents the concentration of the analyte in the calibration fluid, and B represents some altered form or state of A which is not detectable by the sensor assay. The behaviour of this system can be described by a simple first-order differential equation:

$$\frac{dC_A}{dt} = -k_{1fwd} \cdot C_A \tag{19}$$

where C_A is the concentration of the analyte species in the calibration fluid and k_{1fwd} is the reaction rate coefficient for the process. For this work, k_{1fwd} is assumed to have an Arrhenius-type temperature dependency, as described by:

$$k_{1fwd} = k_{1fwd,ref}\, e^{\frac{-E_a}{R}\left(\frac{1}{T} - \frac{1}{T_{ref}}\right)} \tag{20}$$

where T is absolute temperature in Kelvin, E_a is the activation energy of the process, R is the universal gas constant and $k_{1fwd,ref}$ is a the value of the reaction rate coefficient at temperature T_{ref}. Integration of equation (2) yields the analytical solution for the analyte concentration in the calibration fluid, given by:

$$C_A = C_{A(t=0)} \cdot e^{-k_{1fwd} \cdot t} \tag{21}$$

where $C_{A(t=0)}$ is the initial concentration of analyte in the calibration fluid after manufacture, prior to storage at elevated temperatures and t is time.

The model described by equations (20) and (21) was fit to the data from experiments H and I. The resulting model fit is shown in Figure 3.4.
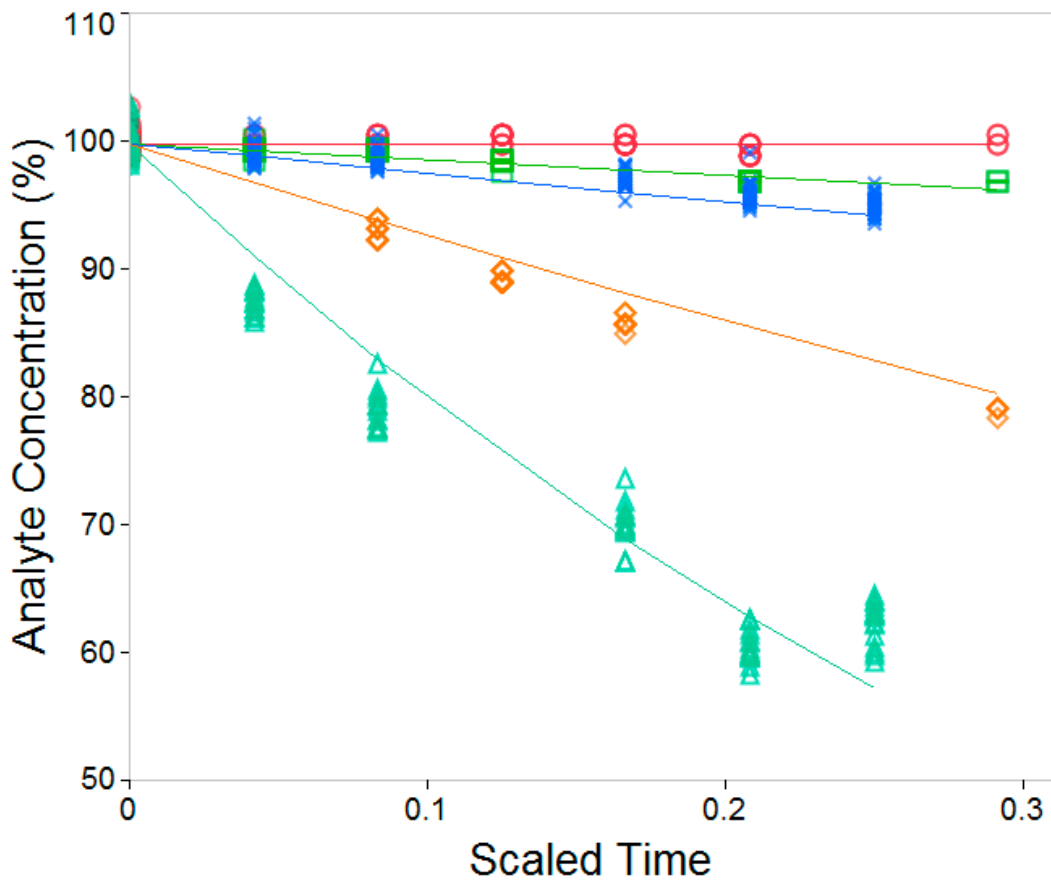
Figure 3.4: First-order model fit to the results of two calibration package incubation experiments (H and I). The storage temperature increased with increasing label number for the storage conditions 1(〇), 2(□), 2a(✕),3(◇) and 4(△).

The first-order model fits the data well, but slightly over-predicts the changes in analyte concentration at storage condition 3. The overall fit seems to capture the key aspects of the observed behaviour. In addition, none of the approximate 95% confidence intervals contain parameter estimates of zero (Table 3.1), indicating that each parameter helps to explain significant trend in the data.

Table 3.1 Parameter estimates and confidence limits for the first-order model fit to calibration package incubation data

Parameter	Estimate	Lower 95% Confidence Limit	Upper 95% Confidence Limit
$k_{1fwd,ref}$	0.000385	0.000303	0.000477
$\dfrac{E_a}{R}$	12100	11300	12900
$C_{A(t=0)}$ (%)	99.8	99.7	100

As mentioned previously, one objective of experiment I was to determine the effect of two other calibration fluid species on the stability of the analyte. The results for this part of the experiment are shown in Figure 3.5.
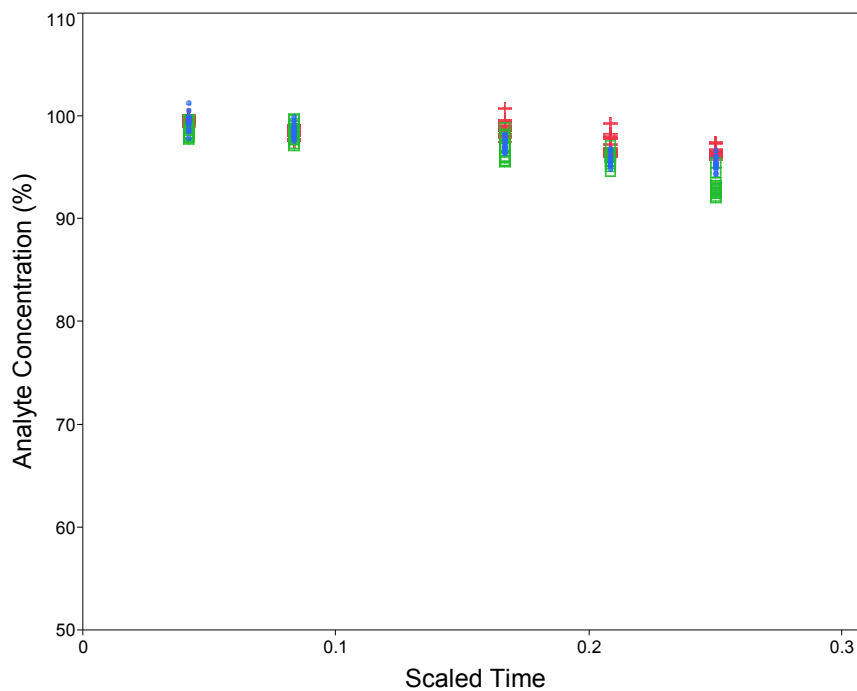
Figure 3.5: Effect of calibration fluid components 1 (+) and 2 (□) on analyte stability, relative to normal calibration fluid (●).

From Figure 3.5 it appears that increasing component 1 appears to slightly slow the rate of change in the analyte concentration while increasing component 2 appears to slightly increase the rate of change of analyte concentration. All three calibration fluid formulations

appear to follow the same general stability behaviour. The changes to the analyte stability due to components 1 and 2 were respectively, less than 1% and 3% of the difference in overall analyte concentration observed in the normal calibration fluid. Since this experiment was carried out at temperatures well above those that a full cartridge would be exposed to under normal storage and use, the mild effect of these components on analyte stability may not be significant enough to warrant further experimental work.

3.6 *Model Validation*

Data from experiments D, E and F were used to test the predictive ability of the model (equations (20) and (21), with parameters from Table 3.1). The model was used to predict the concentration of the calibrant after exposure to different temperatures for different periods of time. These predicted concentrations were used as inputs to the sensor algorithms that compute the measured values of the analyte concentration in the blood sample. The algorithm was used to predict the responses in Figures 3.6-3.8. These predicted responses incorporate both the calibrant signal and the sample signal.
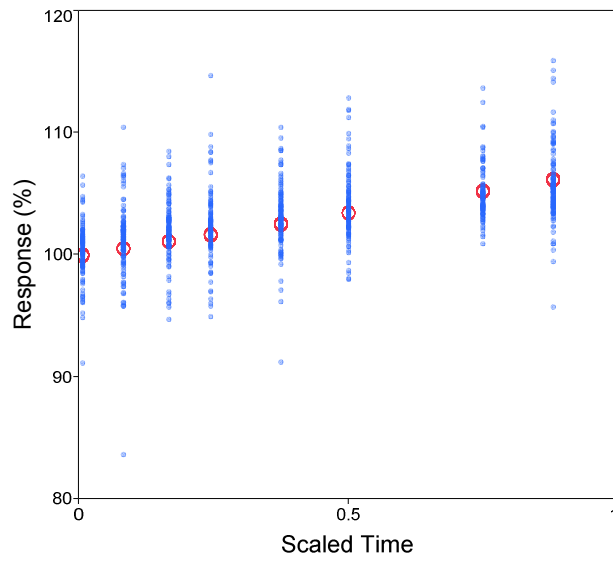
Figure 3.6: Response of whole cartridges from experiment D stored at an elevated temperature equivalent to that of storage condition 2 from experiment H. Experimental data is shown as points (●), model predictions are shown as open circles (O)
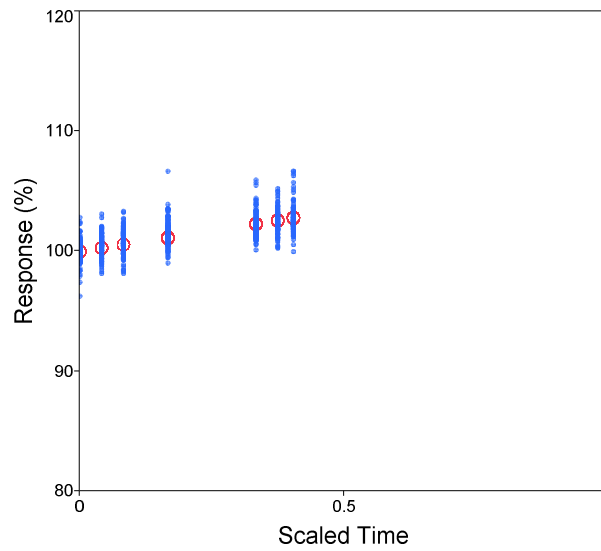
Figure 3.7: Response of whole cartridges from experiment E stored at an elevated temperature equivalent to that of storage condition 2 from experiment H. Experimental data is shown as points (●), model predictions are shown as open circles (O)
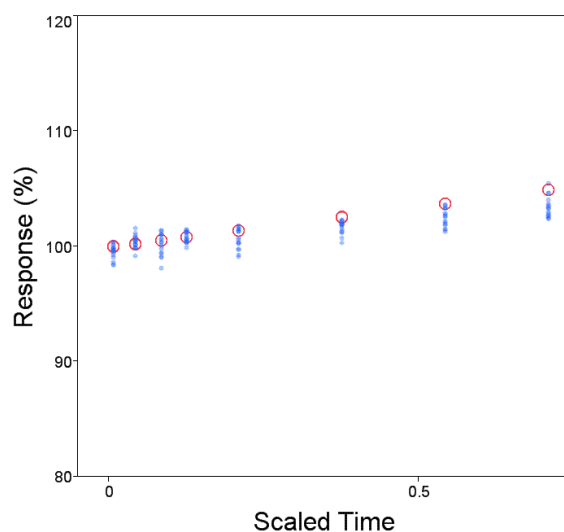
Figure 3.8: Response of whole cartridges from experiment F stored at an elevated temperature equivalent to that of storage condition 2 from experiment H. Experimental data is shown as points (•), model predictions are shown as open circles (O).

Figures 3.6-3.8 show that the stability model for the concentration of the analyte in the calibration fluid can explain the overall upward trend present in the data, across several experiments from production lots. The ability of the first-order model to generate analyte concentration predictions that explain the trend in the data gives some evidence that a changing reference analyte concentration in the calibration package is the dominant process affecting assay stability at the tested thermal exposure levels and durations. Because the first-order model was able to explain the trends in the data, more complex models were not investigated.

3.7   Conclusions

The thermal stability of the reference analyte in the calibration package appears to be an important factor limiting product shelf-life for the assay of interest. A first-order model of analyte stability was developed, which provided an adequate fit of the data for two

experiments that investigate analyte stability in the calibration fluid and span a wide range of elevated temperatures. Parameters estimated from the model fit were all significantly different from zero at the 95% confidence level. These parameters were used to generate predictions of the analyte in the calibration fluid for whole-cartridge incubation experiments. The use of these predictions indicated that the magnitude and form of the changes observed in assay stability could be attributed mainly to changes in concentration of analyte in the calibration fluid. In addition, the effect of two other calibration fluid components on analyte stability were tested, and it was determined that both had a small and negligible effect on the rate of change in analyte concentration over time. Component 1 slowed the change in analyte concentration whereas component 2 acted to increase the rate of change. Both effects were minimal, corresponding to an overall difference in analyte concentration of less than 1% for component 1, and less than 3% for component 2. These effects were observed after storage at condition 2a from experiment I, at which the temperature was significantly higher than the temperatures encountered during normal cartridge use or storage.

This work has implications for design improvements to the assay of interest, as it can be readily extended to the implementation of accelerated testing experiments to test design alternatives in a timely manner. In addition, the model can be used in simulations to explore the current sensitivity of the assay to heating at various temperatures and over different durations, to help improve understanding of the current limitations of the system, and to provide some preliminary indication of how the current storage and shelf-life specifications could be modified without any redesign efforts. Finally, the research has provided evidence supporting the hypothesis that the calibration fluid is the most important stability consideration for the system investigated.

3.8 References (Chapter 3)

[3.1] P. d'Orazio, Biosensors in clinical chemistry, Clin. Chim. Acta 334 (2003) 41-69.

[3.2] P. Boeker, O. Wallenfang and G. Horner, Mechanistic model of diffusion and reaction in thin sensor layers – the DIRMAS model, Sens. Actuators B 83 (2002) 202-208.

[3.3] T. Rinken et al., Calibration of glucose biosensors by using pre-steady state kinetic data, Biosens. Bioelectron. 13 (1998) 801-807.

[3.4] T.D. Gibson, J.N. Hulbert, S.M. Parker, J.R. Woodward and I.J. Higgins, Extended shelf life of enzyme-based biosensors using a novel stabilization system, Biosens. Bioelectron. 7 (1992) 701-708.

[3.5] N.A. Chaniotakis, Enzyme stabilization strategies based on electrolytes and polyelectrolytes for biosensor applications, Anal. Bioanal. Chem. 378 (2004) 89-95.

Chapter 4: Conclusion

4.1 Conclusions and Recommendations

The stability characteristics of two APOC diagnostic assay systems was investigated through the use of mathematical modeling. For each system, available APOC experimental data were analyzed and mathematical models were formulated to describe the stability behaviour of the system. In each case, additional experiments were designed to complement the available experimental data.

For the first assay cartridge investigated (Chapter 2), the sensor had been identified as the most important contributor to overall product stability from previous work by APOC scientists. New experiments were designed and implemented to complement the existing data for parameter estimation, and to produce a data set involving temperature steps for dynamic model validation. A semi-empirical, second-order dynamic model was proposed to describe the stability of the system under varying durations of exposure to elevated temperatures. Conclusions from this study are:

1. The second-order dynamic model showed improved fit for the data sets used for parameter estimation, relative to the fit of a traditional first-order dynamic model. The improved fit is demonstrated by a lower MSE value for the second-order model (2.13×10^{-5} versus 2.69×10^{-5} for the first-order model) and a higher adjusted R^2 value for the second-order model (0.839 versus 0.796). In addition, the results of a mean square ratio test at the 95% confidence level ($F=123 \gg F_{(0.05, 3, 1414)} = 2.61$) provide compelling evidence that the additional terms in the second-order dynamic model explain a significant amount of the variation in the data.

2. The second-order dynamic model demonstrated good predictive ability for the validation data set, which was collected independently of the parameter estimation data sets. The second-order model predictions fall closer to the mean of the sensor activity measurements for each time event, relative to the predictions from the first-order model, which tends to over-predict the sensor activity.

3. Based on conclusions 1 and 2, the thermal stability of the sensor can be better described by a second-order dynamic model than a traditional first-order model.

The extension of the mean kinetic temperature (MKT) concept to second-order and higher-order dynamic systems was explored, by comparing the results from a traditional MKT calculation to an analogous approach developed through simulations and numerical optimization. Identifying an analogous MKT for a second-order dynamic system involved calculating an isothermal temperature that affords the same thermal stress as the variable temperature profile of equal duration, to which the product was exposed. The results of this exploration show that:

4. The traditional form of the MKT calculation, which assumes a first-order model, is not ideal for the sensor investigated. Instead, an analogous MKT calculated from simulations and optimization using the second-order dynamic model provides more accurate results. The discrepancy between the two types of MKT calculations was 1.13 K, for the sensor and dynamic experiment considered in the Chapter 2.

For the second diagnostic assay investigated, the stability concern was not related to the sensor, but rather to a component of the calibration fluid packaged with the assay cartridges. The role of the calibration fluid in assay cartridge stability was hypothesized by APOC scientists following a combination of targeted experimental programs, which investigated components, fluids and sensors. An experiment was designed to complement the existing data for calibration fluid incubation, and a first-order model of analyte stability within the calibration fluid package was developed. Parameters for the first-order model were estimated from two experiments, which involved the incubation of calibration fluid at elevated temperatures. Estimated analyte concentrations for the calibration fluid, predicted from the first-order model, enabled prediction of the stability behaviour observed in whole-cartridge incubation experiments. The results from this research show that:

5. Accurate quantitative predictions of whole-cartridge stability behaviour provide evidence that changes observed for whole-cartridge stability are caused by changes in analyte concentration in the calibration fluid.

4.2   Contributions

The novel contributions of this thesis are:

1. The development of a semi-empirical, second-order dynamic model of sensor thermal stability for one of the APOC assays

2. The extension of the MKT concept to second- (and higher-) order dynamic systems.

3. The development of a first-order dynamic model for the stability of an analyte in the assay calibration fluid for an APOC assay, and the use of this model to explain the stability behaviour of the assay for that specific analyte.

4. The knowledge gained from these contributions will help APOC scientists to extend the shelf-life claims for some of their products. The models will also be helpful for designing accelerating testing protocols for their assays.

4.3 Future Work

The model development process served as a useful tool for exploring causal relationships between stability and assay components; however, to gain the maximum benefit from this work, the proposed models should be applied for shelf-life predictions and accelerated testing extrapolations. These two applications for the models are straightforward extensions of the current work, involving simulations and optimization. Parameter estimates established from short-term accelerated testing can be used with simulations involving long-term storage at normal conditions, to predict product stability over time. Conversely, for simulations at normal storage conditions, the time at which an acceptable confidence bound for the regression line related to the assay stability metric of interest crosses a minimally acceptable stability level threshold would yield an estimate of product shelf-life.

If further time and resources were available to investigate the stability of system components in more detail, fundamental models could be developed for both systems. This would be helpful to precisely identify the components which limit assay stability, and therefore fundamental models would be important guides for assay performance and improvement efforts.

Appendix A: Analytical Solutions

The analytical solution to the second-order model of biosensor stability (equations 5-8, 12) is:

$$Ca\left(t\right) = \frac{1}{2\alpha}\left(\beta \mathrm{e}^{\eta t} - \gamma \mathrm{e}^{\nu t}\right)$$

$$Cb\left(t\right) = \frac{1}{2\alpha k_{1rev}}\left[\left(\beta \eta \mathrm{e}^{\eta t} - \gamma \nu \mathrm{e}^{\nu t}\right) + k_{1fwd}\left(\beta \mathrm{e}^{\eta t} - \gamma \mathrm{e}^{\nu t}\right)\right]$$

where

$$\alpha = \sqrt{k_{1fwd}^{2} + 2\,k_{1fwd}\,k_{1rev} - 2\,k_{1fwd}\,k_{2fwd} + k_{1rev}^{2} + 2\,k_{1rev}\,k_{2fwd} + k_{2fwd}^{2}}$$

$$\beta = \alpha\,Ca0 + k_{2fwd}\,Ca0 + k_{1rev}\,Ca0 - k_{1fwd}\,Ca0 + 2\,k_{1rev}\,Cb0$$

$$\gamma = -k_{1fwd}\,Ca0 + k_{2fwd}\,Ca0 + 2\,k_{1rev}\,Cb0 + k_{1rev}\,Ca0 - \alpha\,Ca0$$

$$k_{1fwd} = k_{1fwdref}\,\mathrm{e}^{-E_{k1fwd}/R\left(T^{-1} - T_{ref}^{-1}\right)}$$

$$\frac{1}{2} \qquad k_{2fwd} = k_{2fwdref}\,\mathrm{e}^{-E_{k2fwd}/R\left(T^{-1} - T_{ref}^{-1}\right)}$$

$$k_{1rev} = k_{1fwd}K_{eq}$$

$$\eta = \left(-\frac{1}{2}\,k_{1fwd} - \frac{1}{2}\,k_{1rev} - \frac{1}{2}\,k_{2fwd} + \frac{1}{2}\,\alpha\right)$$

$$\nu = \left(-\frac{1}{2}\,k_{1fwd} - \frac{1}{2}\,k_{1rev} - \frac{1}{2}\,k_{2fwd} - \frac{1}{2}\,\alpha\right)$$

Appendix B: Experimental Data Testing Plans

Table B1: Experimental testing plan for Data Sets A and B

	# of replicates						
	Data Set A				Data Set B		
	Recoded Temperature (deviation from reference temperature)						
Recoded Event Time (fraction of Data Set A total duration)	-25	-10	0	10	-25	-10	0
0.000	12	0	0	0	50	0	0
0.006	24	24	24	24	32	32	32
0.042	24	24	24	24	0	0	0
0.083	24	24	24	24	32	32	32
0.167	24	24	24	24	32	32	32
0.244	0	0	0	0	32	32	32
0.333	24	24	24	24	0	0	0
0.375	0	0	0	0	32	32	32
0.500	24	24	24	24	32	32	32
0.750	0	0	0	0	32	32	32
0.881	0	0	0	0	32	32	32
1.000	12	0	24	12	0	0	0

Table B2: Experimental testing plan for Data Set C

Recoded Event Time (fraction of Data Set A total duration)	Recoded Temperature (deviation from reference temperature)*	# of replicates
0	10	22
0.042	-25	22
0.083	10	22
0.125	10	22
0.167	10	22

*Note: Temperatures were held constant between test events (e.g. cartridges were stored 25 degrees Kelvin below the reference temperature between events 0.042 and 0.083)

Table B3: Experimental testing plan for Data Sets D, E and F

Recoded Event Time (fraction of Data Set A total duration)	# of replicates							
	Data Set D			Data Set E	Data Set F			
	Recoded Temperature (degrees Kelvin deviation from reference temperature)							
	-25	-10	0	0	-25	-5	0	5
0.000	50	0	0	30	7	0	0	0
0.006	32	32	32	0	8	8	8	8
0.042	0	0	0	30	8	8	8	8
0.083	32	32	32	30	8	8	8	8
0.125	0	0	0	0	8	8	8	8
0.167	32	32	32	30	0	0	0	0
0.208	0	0	0	0	8	8	8	8
0.244	32	32	32	0	0	0	0	0
0.333	0	0	0	30	0	0	0	0
0.375	32	32	32	30	8	8	8	8
0.405	0	0	0	30	0	0	0	0
0.500	32	32	32	0	0	0	0	0
0.542	0	0	0	0	8	8	8	8
0.708	0	0	0	0	8	8	8	8
0.750	32	32	32	0	0	0	0	0
0.881	32	32	32	0	0	0	0	0

Table B4: Experimental testing plan for Data Set G

Recoded Event Time (fraction of Data Set A total duration)	# of replicates
0.006	24
0.042	24
0.083	24
0.167	24
0.333	24
0.500	24
1	12

Table B5: Experimental testing plan for Data Sets H and I

	# of replicates					
	Data Set H			Data Set I		
	Recoded Temperature (degrees Kelvin deviation from reference temperature)					
Recoded Event Time (fraction of Data Set A total duration)	-25	5	20	-25	10	30
0.000	12	0	0		30	30
0.042	12	12	0	0	30	15
0.083	12	12	12	0	30	15
0.125	12	12	12	0	0	0
0.167	12	0	12	0	30	15
0.208	12	12	0	0	30	15
0.250	0	0	0	0	30	15
0.292	12	12	12	0	0	0

Appendix C: Discussion of Experimental Variability

There are several potential sources of variability inherent with the APOC i-STAT cartridge system investigated over the course of this work. This section gives a more detailed description of the aspects of the APOC system that should be accounted for when considering the variability of experimental results.

1. APOC medical diagnostic cartridges are manufactured as single-use devices. As a result, all of the testing performed over the course of this research was destructive testing. Therefore, the results from the experimental data sets have inherent variability between individual cartridges and consist of a separate distribution of experimental observations at each unique testing condition.

2. An APOC diagnostic cartridge is composed of many components which are manufactured separately. Efforts were made during experimental design to keep cartridge and component manufacturing lots the same within each experimental data set. When this was not possible, statistical assessments of differences between mean response values for different lots were performed at matching storage conditions, to ensure that the lot-to-lot differences were negligible.

3. The experimental data sets analyzed over the course of this work varied in their run dates. Several data sets used were older, historical data sets from several years ago, whereas some of the other data sets (including the newly designed data sets) were concluded in parallel with this work. The timing of the experimental data sets in an important consideration as APOC updates coefficients for their products frequently (approximately every 6 months) to account for changes in manufacturing materials and practices (otherwise lot-to-lot differences could become significant). In order to remove the effect of manufacturing date from the results and allow for meaningful comparisons between data sets, the results from each data set were scaled relative to their respective day 0 means. An assumption inherent with this approach is that the experimental "day 0" represents a similar time-from-manufacture estimate across data sets. This is not necessarily a valid assumption, as the post-manufacturing delay for several of the data sets analyzed was large (several days or weeks). However, the cartridges were stored at reduced temperatures for the duration of this post-manufacturing delay in each case and the experimental results indicate insignificant drifts in sensor responses after storage at low temperatures. These two factors were considered when assuming "day 0" responses could be used to scale the data sets for comparison.

4. The aqueous control fluids of known analyte concentrations used for cartridge testing are also susceptible to some lot-to-lot variability. Again, efforts were made to use

control fluids from the same manufacturing lot within experimental data sets. Since these fluids are produced to meet tight specifications in an analytical chemistry laboratory, there was less of a concern for between-lot variations from this source. (post-production testing to ensure that these fluids are within specifications is performed for each control fluid lot and results from these tests were available).
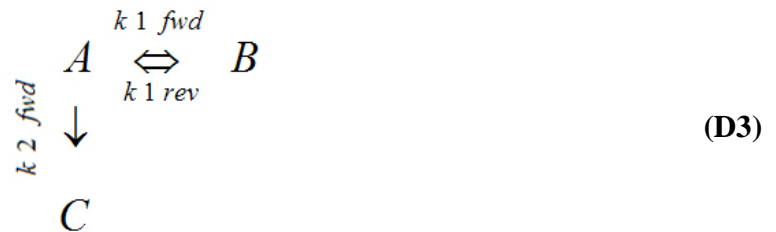
Appendix D: Alternative Modeling Approaches

The model development process applied during this work was an iterative one. As a result, there were several approaches attempted which did not yield the best results, and were therefore discarded. This Appendix section describes some of these approaches which were omitted in the main text for brevity.

1. Alternate forms of second-order dynamic models were also investigated (as alternatives to equation 4).

$$A \underset{k_{1\,rev}}{\overset{k_{1\,fwd}}{\Longleftrightarrow}} B \overset{k_{2\,fwd}}{\longrightarrow} C \qquad (22)$$
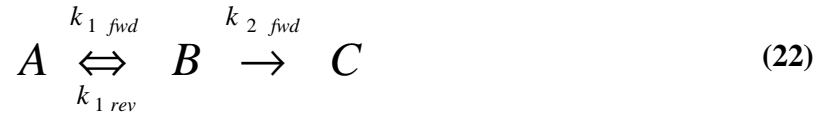
These models took the following forms:

$$A \overset{k_{1\,fwd}}{\longrightarrow} B \overset{k_{2\,fwd}}{\longrightarrow} C \qquad (D1)$$

$$A \overset{k_{1\,fwd}}{\longrightarrow} B \underset{k_{2\,rev}}{\overset{k_{2\,fwd}}{\Longleftrightarrow}} C \qquad (D2)$$

$$\begin{array}{c} A \underset{k_{1\,rev}}{\overset{k_{1\,fwd}}{\Longleftrightarrow}} B \\[2mm] \Big\downarrow \scriptstyle{k_{2\,fwd}} \\[2mm] C \end{array} \qquad (D3)$$

As described in Chapter 2.2.5, "A" is defined as the sensor's native, active state and it is the quantity that is being observed. States "B" and "C" help describe the dynamic behaviour of the sensor and can be loosely considered as different active states of the sensor.

The structure of alternative models D1 and D2 is such that the differential equation used to describe the change in "A" is the same in both cases:

$$\frac{dA}{dt} = -k_{1fwd} \cdot A \qquad \textbf{(D4)}$$

which is identical to the differential equation describing the first-order dynamic model. Neither of these two models (D1 or D2) were investigated further, as the solution for the "A" differential equation is the same as for the previously investigated first-order dynamic system. There is no coupling of "B" or "C" behaviour into the "A" differential equation. In contrast, the reversible transition from "A" to "B" couples the "A" and "B" differential equations, producing a different dynamic response in "A".

The second-order dynamic model in equation D3, was investigated alongside the model from equation 4. Regression experiments using Data Set A consistently showed that the model in equation 4 provided a superior fit in terms of total SSE relative to the model from equation D3. As a result, the model in equation 4 was selected as the second-order dynamic model candidate for this work, and used for fitting Data Sets A and B for parameter estimation and to Data Set C for model validation.

Appendix E: Boxplots for Data Sets A, B, D, E and F
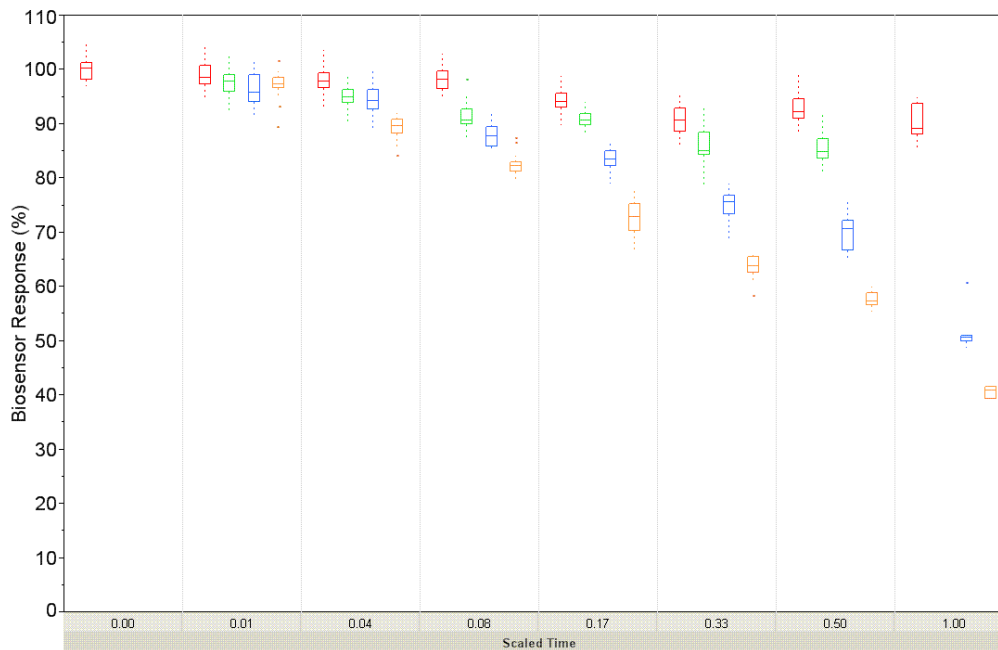
Figure E1: Data Set A - Biosensor response (% of initial activity) versus time for biosensors tested after storage at four different conditions (☐☐☐☐) of increasing temperature (from left to right within each scaled time event). Storage Condition I (☐) corresponds to the lowest temperatures and Storage Condition IV (☐) corresponds to the highest temperatures tested. The time axis has been recoded as a fraction of the total duration of the Data Set A experiment.
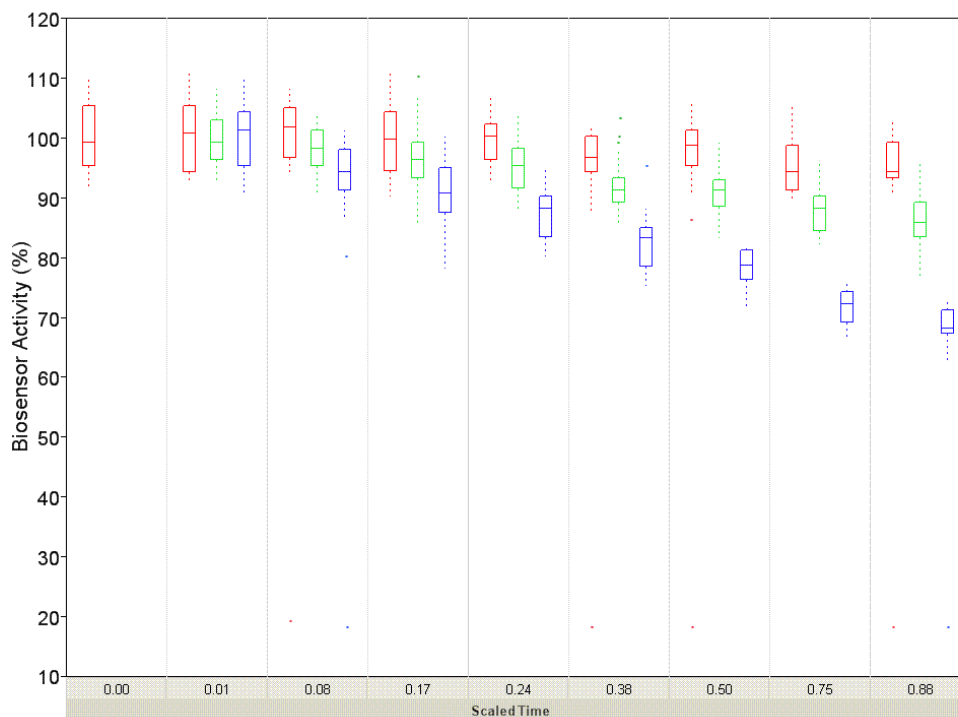
Figure E2: Data Set B - Biosensor response (% of initial activity) versus time for biosensors tested after storage at three different conditions (☐☐☐) of increasing temperature (from left to right within each scaled time event). Storage Condition i (☐) corresponds to the lowest temperatures and Storage Condition iii (☐) corresponds to the highest temperatures tested. The time axis has been recoded as a fraction of the total duration of the Data Set A experiment.
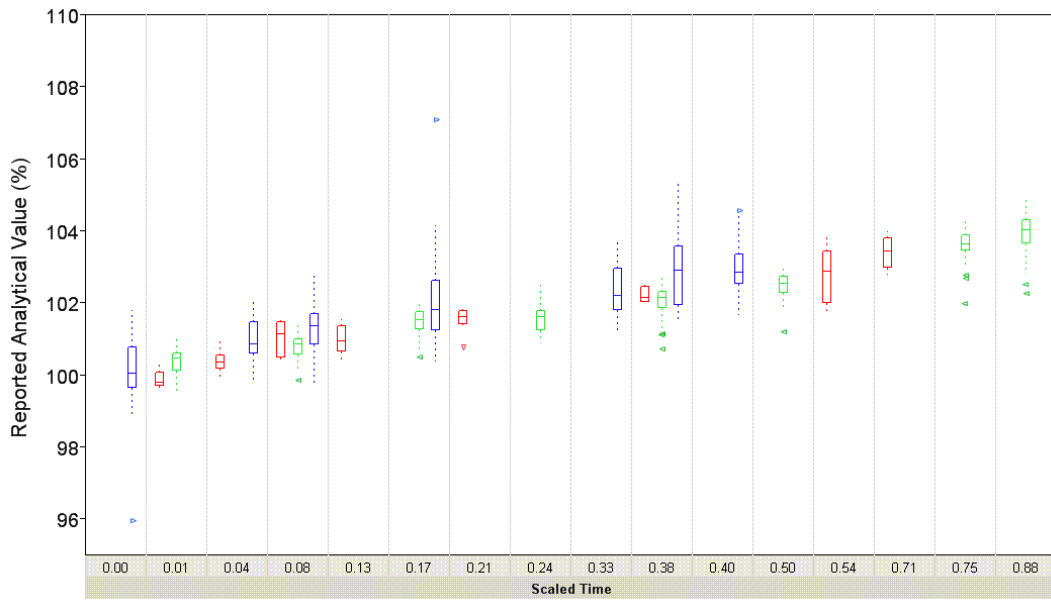
Figure E3: Estimate of analyte concentration from the assay of interest as a percentage of the initial value after storage at an elevated temperature, for Experiments F(☐,▽), E(☐,▷) and D (☐,◁). The time axis has been recoded as a fraction of the longest duration for the experiments.